Revealing the Deformation of SW Anatolia (Turkey) by Anisotropy of Magnetic Susceptibility (AMS) Data

Nuretdin Kaymakcı[1], Murat Özkaptan[2], Erhan Gülyüz[3], Bora Uzel[4], Cor Langereis[5], and A. Arda Ozacar[1]

[1]Middle East Technical University, Department of Geological Engineering, Ankara, Turkey
[2]Karadeniz Technical University
[3]Van Yüzüncü Yıl Üniversitesi
[4]Dokuz Eylül Üniversitesi
[5]Utrecht University

November 23, 2022

Abstract

Convergence between the Eurasian and the African plates in the West Anatolian-Aegean region results in a trench retreat due to slab roll-back and tearing of the subducted African lithosphere. The upper plate response of this process gave way to back-arc extension in the region. In this context, we have conducted a very rigorous AMS study on the Neogene units in SW Anatolia to unravel the style and amounts of deformation. For this purpose, from 83 sites in 11 structurally homogeneous domains, 1680 paleomagnetic samples were analyzed. Obtained results are used to determine principal strain directions to unravel overall deformation styles and amounts in the region.
The results have shown that AMS is related to the tectonic deformation, which facilitated that the AMS directions correspond to cumulative principal strains. Maximum susceptibility is parallel to the major extension (k), minimum susceptibility (k) corresponds to compaction after deposition, almost always normal to the bedding plane. The intermediate axis (k) found to be parallel to a second extension direction that the region has been under the control of multi-directional extension during Neogene.

Two mean anisotropy directions are identified. These are Oligocene-Middle Miocene NW-SE, and Late Miocene-Pliocene NE-SW directed extension. The mean anisotropy directions are generally parallel or perpendicular to the general strikes of the normal faults. The results have shown that the deformation in the region resembles to differentially stretched rubber sheet under the influence of SW directed extension exerted by the southwards retreating Eastern Mediterranean subduction system.

Posted on 23 Nov 2022 | CC-BY-NC 4 | https://doi.org/10.1002/essoar.10503026.1 | This a preprint and has not been peer reviewed. Data may be preliminary.

Revealing the Deformation of SW Anatolia (Turkey) by Anisotropy of Magnetic Susceptibility (AMS) Data

Murat Özkaptan[1], Erhan Gülyüz[2], Bora Uzel[3], Cor G. Langereis[4], Özacar, A.A[5], Nuretdin Kaymakcı[5]*

[1] Karadeniz Technical University, Department of Geophysical Engineering, 61080 Trabzon, Turkey

[2] Van Yüzüncü Yıl University, Department of Geological Engineering, 65080 Van, Turkey

[3] Dokuz Eylül University, Department of Geological Engineering, 35160 İzmir, Turkey

[4] Paleomagnetic Laboratory Fort Hoofddijk, Department of Earth Sciences, Utrecht University, Budapestlaan 17, 3584 CD Utrecht, the Netherlands

[5] Middle East Technical University, Department of Geological Engineering, Dumlupinar Bulvari No. 1, 06800 Ankara, Turkey ORCID:0000-0002-7618-0226

Corresponding author: Nuretdin Kaymakci (kaymakci@metu.edu.tr)

Key Points:

- AMS data from SW Anatolia revealed the amount and orientations of principal strains.
- The SW Anatolia underwent NW-SE, and NE-SW directed extension in the Oligocene-Middle Miocene and Late Miocene-Pliocene, respectively.
- Deformation is the result of SW directed stretching of the over-riding plate above southwards retreating subducted African oceanic slab.

Abstract

Convergence between the Eurasian and the African plates in the West Anatolian-Aegean region results in a trench retreat due to slab roll-back and tearing of the subducted African lithosphere. The upper plate response of this process gave way to back-arc extension in the region. In this context, we have conducted a very rigorous AMS study on the Neogene units in SW Anatolia to unravel the style and amounts of deformation. For this purpose, from 83 sites in 11 structurally homogeneous domains, 1680 paleomagnetic samples were analyzed. Obtained results are used to determine principal strain directions to unravel overall deformation styles and amounts in the region.

The results have shown that AMS is related to the tectonic deformation, which facilitated that the AMS directions correspond to cumulative principal strains. Maximum susceptibility is parallel to the major extension (k_{max}), minimum susceptibility (k_{min}) corresponds to compaction after deposition, almost always normal to the bedding plane. The intermediate axis (k_{int}) found to be parallel to a second extension direction that the region has been under the control of multi-directional extension during Neogene.

Two mean anisotropy directions are identified. These are Oligocene-Middle Miocene NW-SE, and Late Miocene-Pliocene NE-SW directed extension. The mean anisotropy directions are generally parallel or perpendicular to the general strikes of the normal faults. The results have shown that the deformation in the region resembles to differentially stretched rubber sheet under the influence of SW directed extension exerted by the southwards retreating Eastern Mediterranean subduction system.

Plain Language Summary

The tectonic style and amount of crustal deformation in SW-Anatolia are revealed by rigorous Anisotropy of Magnetic Susceptibility (AMS) data obtained from SW Anatolia. It is found that the orientation of principal strain axes change gradually while the shape of the strain ellipsoid among all the Late Miocene-Pliocene domains remain the same. Based on these results and published information, we conclude that the SW Anatolia is under the control of multi-directional extension associated with counterclockwise rotation exerted by the southwards retreat of the Eastern Mediterranean subduction system (Hellenic-Pliny-Sratbo and Cyprian Trenches). The retreat resulted in stretching of the SW Anatolia, the over-riding plate, to accommodate the retreat of the trench as a non-rigid, stretched rubber-sheet like deformation style (Figure 9), which seems to be pulled from a single point towards SW. The Büyük Menderes-Denizli-Baklan grabens and Dinar-Aksu faults mark the northern boundary of this peculiar deformation zone.

1 Introduction

The Anisotropy of Magnetic Susceptibility (AMS) of detrital material determines the magnetic fabric of magnetic grains in a rock volume, and it is directly related to deformation; hence the strain ellipsoids. The shape is primarily controlled by primary geological processes such as paleocurrent patterns that produce purely sedimentary magnetic fabric; however, secondary factors such as compaction and tectonic deformation are the important factors on the development of the magnetic fabric. Discrimination between the primary and secondary (post-depositional) factors is very crucial in the utilization of AMS ellipsoid as a strain marker. Classical methods for the determination of strain ellipsoids for sedimentary rocks involves clast-based measurements such as clast geometry, orientations, texture, and packing (Ramsey & Huber, 1983). However, AMS-based strain determination techniques in low to mildly deformed sedimentary rocks provide quantification of principal strain axes using the magnetic grains located in rock volumes (Borradaile & Henry, 1997; Hirt et al., 1993; Parés & van der Pluijm, 2002; Sagnotti & Speranza, 1993).

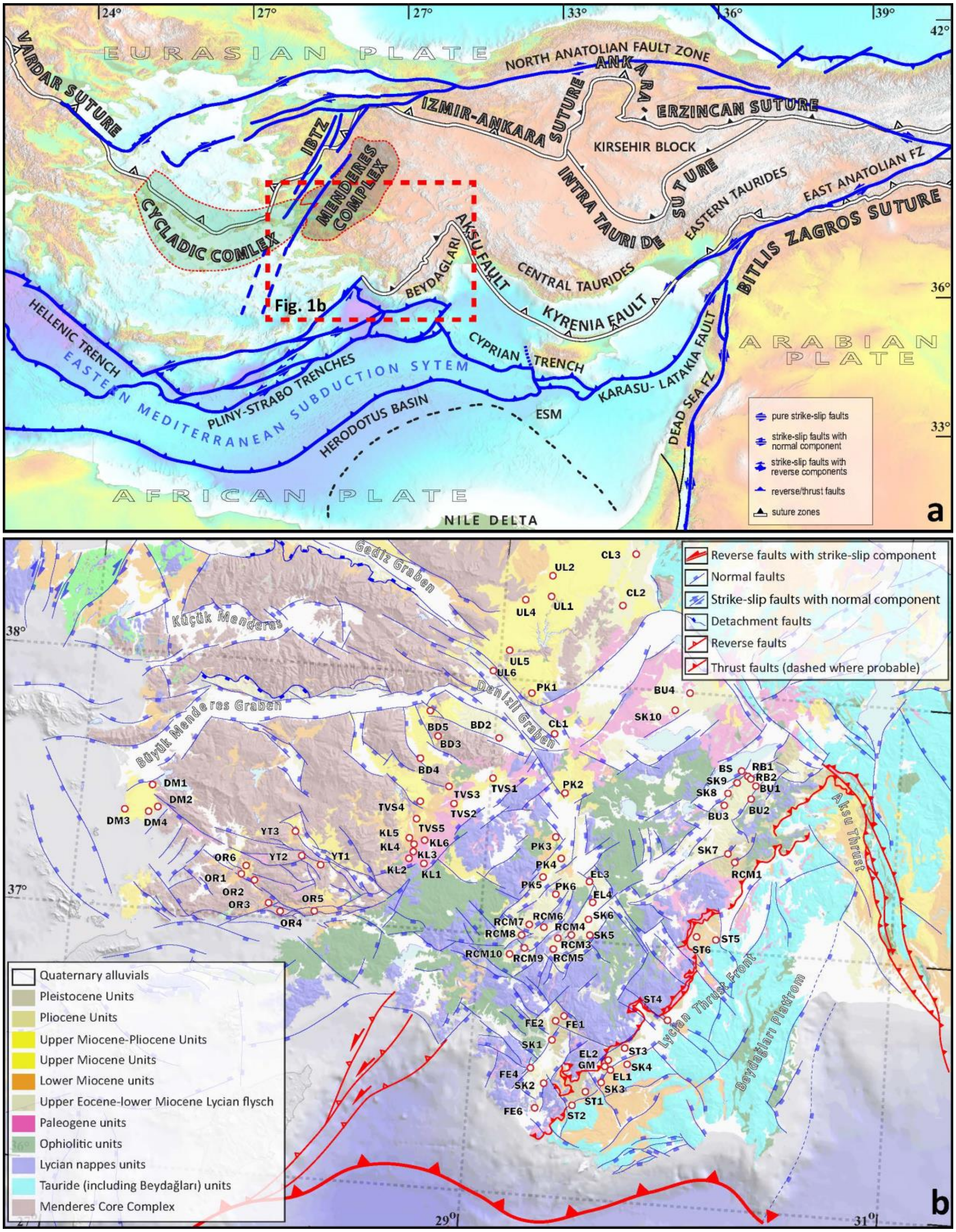

Figure 1. a) Simplified tectonic scheme of the eastern Mediterranean region. b) simplified geological map of SW Anatolia showing AMS sample locations and major faults (MTA, 2002 and Kaymakcı et al., 2018).

Deformation related to tectonic processes is mainly recorded in sedimentary basins. Deciphering these records helps to understand the basic geological/tectonic processes that have acted upon the rock, although quantitatively describing the records is not always possible by using classical geological tools such as grain-based techniques, especially in the case of lack of penetrative deformation. Although, paleostress analyses conducted directly on fault surfaces provide clues about the strain axes; however, they are always discrete and resulted from inhomogeneous deformation, which does not always reflect the regional strain ellipsoid. The AMS technique, on the other hand, is an alternative and effective method for the determination of strain ellipsoid in low to mildly deformed sedimentary rocks. Care must be given to the fact that the minor strain axis almost always corresponds to compaction (Duermeijer et al., 1998).

In this regard, this paper documents a very detailed AMS data to quantify and unravel deformation styles in the late Oligocene - Neogene basins in SW Anatolia where rotational extensional deformation has been taken place (Kaymakcı et al., 2018) related to slab edge processes at the over-riding plate of the Aegean-Cyprian subduction system. These basins include Acıpayam, Burdur, Çameli, Denizli, Elmalı, Ören and Tavas basins (Figure 1), which have infills with a continental origin, and they; (i) spatially cover almost whole SW Anatolia where the Menderes Core Complex, Lycian Nappes, and Tauride Platform rocks are exposed, and (ii) temporally cover the Oligocene to Pliocene time interval, which includes the exhumation of the Menderes Core Complex, emplacement of the Lycian Nappes and subduction history of the African oceanic lithosphere along the eastern Mediterranean trenches (Figure 1; Alçiçek, 2007; Alçiçek et al., 2013; Biryol et al., 2011; Hayward, 1984; van Hinsbergen, Dekkers, et al., 2010; Le Pichon & Angelier, 1979).

Except for the senses and amounts of Neogene rotations in the region (e.g., van Hinsbergen, Dekkers, et al., 2010; Kaymakcı et al., 2018), the studies concerned with the quantification of deformation amounts and the strain related to the ongoing tectonic processes in the region are relatively rare. There are few studies which are concerned about the temporal and tectonostratigraphic records of these geological processes, but they are constrained only a few basins in the region or are based on regional correlations of the stratigraphic sequences (Alçiçek et al., 2019; Kaymakcı, 2006; Özkaptan et al., 2018 and references therein).

Seismic tomographic studies have shown that the subducted African oceanic slab is fragmented in the mantle (Biryol et al., 2011; Faccenna et al., 2006; van Hinsbergen, Kaymakcı, et al., 2010) and gave way to differential stretching on the over-riding plate of SW Anatolia and the Aegean region (Figure 1). Related to this issue, one of the hottest debates are related to the surface expressions of the fragmented African slab in SW Anatolia. It is generally accepted that the fragmented subducted slab below the SW Anatolia developed a tear that provided a mantle window below western Anatolia (Biryol et al., 2011; Faccenna et al., 2006; Govers & Wortel, 2005; Kaymakcı et al., 2018; Wortel & Spakman, 2000). Some studies argued that this tear is coupled with the over-riding plate and produced a large sinistral strike-slip shear zone in SW Anatolia (e.g., Elitez et al., 2016; Elitez & Yaltırak, 2016; Hall et al., 2014). Others, however, claimed that there is no convincing kinematic data obtained from the region to corroborate the presence of a sinistral strike-slip shear zone in the region. Some recent studies (e.g., Alçiçek, 2015; Kaymakcı et al., 2018; Özkaptan et al., 2014, 2018) have shown that SW Anatolia is deforming under a very strong extensional deformation coupled with a regional counterclockwise rotation. Rotation amounts and senses in SW Anatolia is increasing from east to west and north to south, and there is no change in the rotation amounts and senses along the alleged shear zone. Based on this information, Kaymakcı et al. (2018) argued that the subducted slab and the overriding plate are not coupled to produce a continuous shear zone from the mantle up to the surface. In other words, the slab tear in the northern edge of the subducted portion of the African slab does not penetrate the overriding plate, but it is responsible for the distributed differential extensional strain in the region. The differential retreat of the segmented subducted African Slab in the mantle is expressed in the form of rotational (counterclockwise) and extensional deformation on the SW Anatolian crust (Kaymakcı et al., 2018; Özkaptan et al., 2014).

In this contribution, we will shed some light on the kinematic evolution of SW Anatolia based on newly acquired AMS data collected from the Oligocene - Neogene basins in the region. The data covers Oligocene to Pliocene sedimentary records of SW Anatolian basins, and which are constrained temporally by newly established biostratigraphic data of Alçiçek et al., (2019). The main purpose of this study is to quantify the amounts of total cumulative deformation in the region and to establish the principal strain axes in the Neogene deposits in the region based on AMS data.

2 Methods

2.1 Sampling

More than 2000 oriented rock cores for paleomagnetic purposes were drilled in 11 domains consisting of a total of 83 sites in SW Anatolia. Samples were taken both in Eocene-Oligocene (*11 sites/519 cores*) and Miocene (49 sites/ 883 cores) marine sediments (limestones, marls, sandstones) as well as in Miocene to Pliocene (23 sites/ 736 cores) lacustrine to continental clastic rocks (mudstones, claystone, siltstones) (Figure 1). In all sampling locations, the weathered surface was removed to reach fresh sediments. Care was taken to sample away from active faults and other possible disturbance (e.g., chemical or volcanic) near the sampled sites. The standard cylindrical samples (25 mm Ø) were obtained using a handheld gasoline-powered motor drill or an electric drill with a generator, depending on the rock type in the sites, both equipped with water-cooled diamond-coated drill bits. Both core orientations and bedding attitudes were always measured in the field using a magnetic compass, later corrected for the present-day declination (4.5°W for the entire sampling period, June 2013). Drilled sample cores were marked, wrapped in aluminum foil, and put in protective plastic bags. Since the collected samples were used for various paleomagnetic purposes (determining tectonic vertical axis block-rotations as well as magnetostratigraphy), the number of samples taken per site is variable; a minimum of 13 but - at some localities for magnetostratigraphy – it can reach a maximum of ~400 samples. Ages of the sampled lithologies are adopted from Kaymakcı et al. (2018) and Konak & Şenel (2002), Şenel (2002).

2.2. Thermomagnetic experiments

Before the AMS measurements, at least one thermomagnetic measurement was carried out for each sample location in order to determine the characteristics of the magnetic minerals in the rock samples. Thermomagnetic runs were carried out in the air, and the total magnetic moment versus temperature (M/T) diagrams was obtained using a modified horizontal translation type Curie-balance with a sensitivity of ~5 x 10^{-9} m^2 (Mullender et al., 1993, 2016). Depending on the expected dominant rock magnetic mineral intensity, approximately 50-100 g of powdered material from one specimen in each site was put into a quartz glass sample holder and held in place by quartz wool. We used several heating-cooling cycles that were used up to successively higher temperatures (max. 700°C), finally cooling down to 20°C (room temperature). The successive heating and cooling rates were 10°C/min in air. Based on the thermomagnetic curves, Curie temperatures were determined following (Fabian et al., 2013). At least one thermomagnetic experiment was performed for each of 83 locations, but one representative curve for each of the 11 identified domains is illustrated in Figure 2.

2.3 AMS measurements

The collected samples were cut to standard specimen sizes with a dual blade rock saw (ASC Scientific). Because the AMS results are more affected by shape parameters than the other paleomagnetic methods, only unbroken, crack-free, and whole specimens were prepared for AMS measurements. Generally, the cores collected from the field were sufficiently long to provide more than one standard sample, increasing the number of specimens that can be measured. Optimum height/diameter ratio for specimen sizes varies between 0.8 – 0.9 (Collinson, 1983; Noltimier, 1971; Scriba & Heller, 1978). In total, more than 2000 samples were collected from the field, but only 1680 of them were measured in the AMS analyses due to the reasons mentioned above (Table 1). The AMS specimens were measured with an automatic field variation (low field, 200 A/m) susceptometer using the Multi-Function Kappabridge MFK1-FA (AGICO-Brno, Czech Republic), equipped with an up-down mechanism and a rotator. The measurement sensitivity is 10^{-8} SI, which is very critical for some sedimentary rocks (especially limestones), which exhibit very weak magnetic magnetization properties. All measurements and analyses were conducted at the Fort Hoofddijk Paleomagnetic Laboratory of Utrecht University (The Netherlands). Anisoft 4.2 data browser (Chadima & Jelinek, 2009) was used for the display of AMS results and their density distributions by converting from specimen coordinates to geographic and tectonic coordinates (tilt corrected). The site mean AMS parameters were calculated according to Jelinek statistics (Jelínek, 1977, 1978), and tilt corrected results are given in Table 1.

2.4 Deformation and anisotropy of magnetic susceptibility

Since the latest few decades, the magnetic fabric of the magnetically-dominant minerals in a rock matrix have been increasingly used as a rock deformation indicator, especially in sedimentary basins (e.g., Borradaile, 1991; Hrouda, 1991, 1993; Maffione et al., 2012; Özkaptan & Gülyüz, 2019; Parés et al., 1999; Sagnotti et al., 1994; Soto et al., 2009; Tarling & Hrouda, 1993). The magnetic fabric orientations of the AMS tensor can often unravel the deformation history of sedimentary rocks, even without observing clear surface indicators for the low to moderate deformed areas (e.g., Cifelli et al., 2004, 2005; Graham, 1966; Hirt et al., 1995; Kissel et al., 1986; Kodama, 1995; Mattei et al., 1997).

The AMS susceptibility ellipsoid can be described by a tensor, which is defined by three principal axes; $k_1 \geq k_2 \geq k_3$ describe maximum, intermediate, and minimum susceptibility, respectively (Hrouda, 1982). The shape of the magnetic deformation ellipsoid is controlled by a combination of these three principal susceptibility vectors. In terms of structural observations, previous AMS studies commonly inferred that in compressional settings the k_1 axis orients perpendicular to the shortening direction and (sub)parallel to fold axes or thrusts strikes, while k_3 remains normal to the bedding plane (Borradaile & Henry, 1997; Maffione et al., 2015; Mattei et al., 1997; Özkaptan & Gülyüz, 2019). However, in extensional settings, the magnetic lineation vector (k_1) coincides with the bedding strike and stretching direction, and is perpendicular to local normal faults (Cifelli et al., 2005; Sagnotti et al., 1994; Soto et al., 2009).

In addition to three susceptibility vectors, several parameters have been used to quantify the degree of the anisotropy and to visualize shape features, with characteristics that are closely related to lithological features and tectonic deformation. The most commonly used ones are:

- k_m (mean magnetic susceptibility) = $(k_1 + k_2 + k_3)/3$,
- P_j (corrected anisotropy degree) = $\exp\{2[(n_1 - n)\,2 + (n_2 – n) + (n_3 - n)\,2]\}^{1/2}$,
- L (magnetic lineation) = k_1/k_2
- F (magnetic foliation) = k_2/k_3
- T (shape parameter) = $(2n_2 - n_1 - n_3)/(n_1 - n_3)$

where, $n_i = \ln k_i$, $n = (n_1 + n_2 + n_3)/3$, proposed by Jelinek, (1981).

k_m provides qualitative and quantitative information about the magnetic (ferromagnetic, paramagnetic, diamagnetic) mineral composition; P_j corresponds to the degree of alignment of the magnetic minerals as a function of strain intensity or magnetic mineralogy that is linear to the bulk susceptibility (Borradaile, 1988; Parés & van der Pluijm, 2002); T gives information about to the shape of the susceptibility ellipsoid varying between prolate (–1) and oblate (1). All the measurements were corrected for bedding attitude, and AMS parameters at both the specimen and site-level were computed following the Jelinek statistics (Jelínek, 1977, 1978).

3 Results

3.1. Thermomagnetic curves

Examples of thermomagnetic runs from 11 different domains, and variable lithologies of Oligocene to Pliocene age are illustrated in Figure 2. In general, the sampled lithologies have a various magnetic carrier(s) in each site, and thermomagnetic curves from these analyses present a moderately high total magnetization typically in the range 1 - 3 x 10-6Am2 for the white marls, mud-siltstones, and limestones, whereas some grey marls and sandstone dominated lithologies are stronger, in the range 7 - 30 x 10-6Am2. Most curves are fully reversible up to 300°C. Above 350°C, there is a general loss of magnetization likely due to oxidation of the available magnetite or some maghemite. The final cooling curve is significantly lower than the heating curves, indicating progressive oxidation of magnetite at the highest temperatures (700°C). Most curves show a Curie temperature of 550-580°C, indicative of the Ti-poor magnetite. Some samples have a smooth decrease and an inflection in magnetization between 300–400°C compatible with some maghemite (Dankers, 1978). Some curves for clay-sandstone, siltstone or mudstone (BU2, RCM7, OR1 in Figure 2) show a strong increase starting at ~400°C which is typically an indicator for the presence of pyrite which is transformed to magnetite during thermal demagnetization, and the newly formed magnetite is subsequently demagnetized or oxidized at ~550°C (Passier et al., 2001).

Table 1. Early Miocene to Pliocene anisotropy of magnetic susceptibility results from the SW Anatolia.

Locality	***Site***	***Geog. Coord. (deg)***		***N_{AMS}***	***Age***	***Rock***	***Bedding***	***$k_{m*}10^{6}$***	***L***	***F***	***Pj***	***T***	***NTC***			***TC***			**e_1**	**e_2**	**e_3**
		Lat. (N)	***Long. (E)***				***Strike/dip***	***(SI)***					***D/I (k_{max})***	***D/I (k_{int})***	***D/I (kMio.n***	***D/I (k_{max})***	***D/I (k_{int})***	***D/I (kMio.***			
Acıpayam	~~PK2~~	~~37.5845~~	~~29.3505~~	~~16~~	~~Plio.~~	~~mud-marl~~	~~193/18~~	~~-0005.7~~	~~1.086~~	~~1.079~~	~~1.181~~	~~0.045~~	~~058.9/42.3~~	~~299.1/28.6~~	~~187.3/34.3~~	~~043.0/53.5~~	~~297.4/11.2~~	~~199.7/34.3~~	~~45.2~~	~~54.5~~	~~50.0~~
	PK3	37.4199	29.3424	09	Plio.	mud-marl	193/18	0082.0	1.005	1.005	1.010	0.030	189.6/05.6	283.9/37.0	092.3/52.4	191.5/06.4	283.7/19.0	083.8/69.8	31.8	29.5	28.2
	PK4	37.3402	29.3659	13	Plio.	mud-marl	252/10	3240.0	1.007	1.014	1.021	0.250	244.7/04.8	335.0/03.9	103.6/83.8	245.6/06.0	155.0/06.1	020.1/81.4	19.3	35.7	33.1
	EL3	37.2308	29.5361	05	Plio.	mud-marl	138/23	4660.0	1.004	1.011	1.015	0.413	063.3/05.4	154.4/11.7	308.9/77.1	065.2/27.5	157.5/04.5	256.0/62.1	20.5	20.7	06.5
	EL4	37.1866	29.5324	06	Plio.	mud-marl	188/08	5990.0	1.007	1.078	1.095	0.783	275.3/11.8	06.5/05.8	122.1/76.8	275.4/03.8	005.7/05.5	150.7/83.3	47.5	47.5	04.4
Plio.	**mean**			33	Plio.			3100.0	1.006	1.022	1.031	0.312	237.1/05.3	327.9/08.8	116.31/79.7	239.7/0.4	329.7/03.5	143.8/86.5	42.1	42.4	16.6
Burdur	BU1	37.6848	30.3129	08	Plio.	mud-marl	090/20	0040.8	1.008	1.009	1.017	0.058	233.5/29.4	141.6/03.4	045.6/60.3	226.9/16.5	320.6/12.2	085.4/69.2	62.1	62.3	31.0
	BU2	37.6218	30.2732	10	Plio.	mud-marl	070/20	0174.0	1.007	1.024	1.033	0.481	245.7/13.2	155.2/02.0	057.0/76.6	241.4/11.0	335.0/18.0	121.5/68.8	18.5	18.8	07.2
	BU3	37.5796	30.1568	06	Plio.	mud-marl	355/19	0076.5	1.003	1.015	1.020	0.663	293.4/11.0	023.9/02.7	127.5/78.6	296.7/27.5	203.3/6.5	101.2/61.6	33.0	32.8	09.1
	RB1	37.7074	30.2925	15	Plio.	mud-sand.	043/11	0012.0	1.019	1.024	1.045	0.167	234.7/11.9	144.5/00.6	051.6/78.1	232.2/13.8	324.7/10.2	089.8/72.7	23.9	23.9	07.5
	RB2	37.7074	30.2925	07	Plio.	mud-sand.	040/16	0031.4	1.008	1.023	1.033	0.439	067.1/02.3	337.0/00.3	239.0/87.7	246.7/05.0	138.3/74.6	138.3/74.6	11.8	13.0	07.5
	SK7	37.4861	30.1595	18	Plio.	mud-marl	036/16	0092.2	1.003	1.020	1.026	0.685	090.0/08.7	180.7/04.4	297.4/80.3	270.4/04.3	000.7/04.9	138.9/83.5	18.2	18.4	07.4
	SK8	37.6389	30.1677	09	Plio.	mud-marl	312/05	0080.8	1.003	1.017	1.021	0.705	131.1/08.9	040.5/04.1	286.2/80.2	130.3/08.8	220.5/00.9	316.5/81.2	65.3	65.3	11.2
	~~SK9~~	~~37.7053~~	~~30.2379~~	~~08~~	~~Plio.~~	~~mud-marl~~	~~035/20~~	~~0006.7~~	~~1.036~~	~~1.027~~	~~1.064~~	~~-0.137~~	~~136.2/12.8~~	~~229.9/15.8~~	~~008.9/69.5~~	~~136.2/12.8~~	~~223.5/19.9~~	~~064.1/68.9~~	~~54.8~~	~~67.3~~	~~67.4~~
	RCM1	37.4689	30.1794	10	Plio.	mud-clay	070/20	0109.0	1.002	1.018	1.022	0.830	100.9/04.9	192.7/20.1	357.9/69.3	280.8/05.5	190.5/03.0	071.8/83.7	23.1	23.2	07.8
	BS	37.7071	30.2926	114	Plio.	mud-marl	070/10	0049.8	1.007	1.019	1.028	0.399	110.9/10.4	201.5/03.2	308.7/79.1	111.6/03.7	021.3/03.7	246.7/84.8	54.5	54.6	15.1
Plio.	**mean**			197	Plio.			0061.3	1.007	1.019	1.028	0.446	083.5/02.7	173.8/07.7	334.2/81.8	258.6/02.2	348.7/02.3	124.9/86.8	70.3	70.3	14.4
Çameli	RMC3	37.0369	29.4547	20	Lt. Mio.-Plio.	clay-sand.	130/10	0010.4	1.043	1.023	1.072	-0.005	098.3/21.7	358.1/24.1	225.4/56.6	102.2/26.7	354.5/31.3	224.3/46.6	47.2	60.0	60.0
	RCM4	37.0236	29.3859	23	Lt. Mio.-Plio.	mud-marl	220/10	0009.1	1.011	1.011	1.023	-0.023	163.4/22.8	256.8/08.1	005.3/65.6	164.7/26.9	257.3/05.1	357.2/62.5	20.6	56.5	56.2
	RCM5	36.9765	29.3600	17	Lt. Mio.-Plio.	mud-marl	220/05	0325.0	1.004	1.008	1.013	0.178	233.7/07.6	324.1/03.2	077.2/81.8	234.4/04.3	144.1/04.1	011.0/84.1	36.7	37.2	20.9
	RCM6	37.0718	29.3126	59	Lt. Mio.-Plio.	clay	210/08	0035.2	1.004	1.015	1.020	0.612	161.9/09.4	068.9/12.9	287.2/74.0	160.9/04.3	070.6/04.4	295.4/83.8	44.5	44.5	07.6
	RCM7	37.0602	29.2394	24	Lt. Mio.-Plio.	clay	012/10	0066.1	1.004	1.018	1.024	0.659	044.4/01.5	314.3/02.4	165.8/87.1	224.4/04.2	314.7/04.2	089.7/84.0	10.5	10.5	05.7
	RCM8	37.0263	29.0185	30	Lt. Mio.-Plio.	clay-sand.	332/06	0061.9	1.002	1.014	1.017	0.703	266.1/17.9	011.0/17.9	156.6/46.0	277.1/13.4	007.5/01.6	104.3/76.5	30.8	31.0	09.1
	RCM9	36.9768	29.2231	35	Lt. Mio.-Plio.	clay	265/38	0016.4	1.012	1.018	1.031	0.218	048.9/48.1	155.0/13.9	256.3/38.5	054.2/09.1	145.9/10.6	284.4/76.0	25.6	25.7	13.8
	RCM10	36.9482	29.1491	43	Lt. Mio.-Plio.	clay	335/40	0067.9	1.007	1.010	1.017	0.193	086.2/19.5	182.3/16.9	310.3/63.7	268.2/0.1	178.2/05.7	359.4/84.2	11.1	11.1	06.1
	PK5	37.2315	29.3070	10	Lt. Mio.-Plio.	mud-marl	350/18	2320.0	1.003	1.014	1.018	0.486	280.5/12.3	011.3/03.3	116.2/77.2	283.1/29.1	191.3/03.2	095.5/60.7	29.7	30.9	20.9
	PK6	37.2099	29.3488	07	Lt. Mio.-Plio.	mud-marl	345/10	0069.3	1.004	1.004	1.008	0.132	107.0/12.9	016.8/01.0	282.5/77.1	106.2/04.3	196.5/04.3	330.9/83.9	49.6	49.4	31.0
	SK5	37.0444	29.5360	17	Lt. Mio.-Plio.	mud-marl	356/29	0146.0	1.005	1.006	1.010	0.093	051.8/14.8	143.8/07.5	259.7/73.3	047.9/01.8	324.0/08.2	094.3/77.5	24.9	30.8	29.6
	SK6	37.1036	29.5265	17	Lt. Mio.-Plio.	mud-marl	320/08	0059.5	1.006	1.009	1.016	0.211	044.7/20.6	312.7/05.4	208.8/68.7	045.0/12.6	313.5/06.3	197.5/75.9	59.6	59.6	14.3
Lt. Mio.-Plio.	**mean**			295	Lt. Mio.-Plio.			0143.0	1.006	1.012	1.019	0.347	048.2/15.0	140.8/09.3	261.6/72.2	056.0/00.3	146.0/02.7	319.8/87.3	64.4	64.4	17.5
Denizli	BD2	37.8168	28.8638	05	Lt. Mio.	marl	028 / 16	0104.0	1.002	1.018	1.022	0.784	126.6/10.3	036.3/01.6	297.3/79.6	306.5/05.5	216.4/00.7	119.4/84.4	19.1	19.1	03.1
	~~BD3~~	~~37.7699~~	~~28.7296~~	~~12~~	~~L.Mio.~~	~~marl~~	~~118 / 22~~	~~0131.0~~	~~1.005~~	~~1.006~~	~~1.012~~	~~-0.029~~	~~213.4/26.3~~	~~119.2/08.4~~	~~013.0/62.2~~	~~212.8/04.3~~	~~122.3/07.3~~	~~333.4/81.5~~	~~52.1~~	~~56.7~~	~~52.2~~
	BD4	37.7329	28.6304	16	Lt. Mio.	marl	+	0023.6	1.010	1.014	1.025	0.183	271.7/06.3	002.3/05.5	132.9/81.6	ii	002.3/05.5	132.9/81.6	54.8	54.5	24.4
	BD5	37.8621	28.6718	10	Lt. Mio.	marl	136 / 24	1330.0	1.018	1.058	1.080	0.536	165.1/01.8	255.6/15.4	068.7/74.5	343.6/09.8	074.6/05.7	194.2/78.7	42.2	42.2	05.2
Lt. Mio.	**mean**			31	Lt. Mio.			0459.0	1.011	1.029	1.042	0.394	331.2/02.0	240.8/10.3	331.2/02.0	326.1/07.7	056.7/04.8	178.3/80.9	70.1	70.1	10
Didim	~~DM1~~	~~37.4776~~	~~27.3436~~	~~25~~	~~Plio.~~	~~lmst~~	~~024/12~~	~~0024.1~~	~~1.104~~	~~1.069~~	~~1.207~~	~~0.055~~	~~147.5/19.9~~	~~258.4/44.6~~	~~040.6/38.7~~	~~145.8/09.8~~	~~249.4/53.9~~	~~049.0/34.4~~	~~29.4~~	~~34.5~~	~~30.1~~
	~~DM2~~	~~37.4127~~	~~27.3755~~	~~27~~	~~Plio.~~	~~lmst~~	~~002/07~~	~~-0006.4~~	~~1.050~~	~~1.033~~	~~1.100~~	~~-0.051~~	~~111.9/03.4~~	~~020.3/26.1~~	~~208.7/63.7~~	~~291.9/03.2~~	~~023.3/23.7~~	~~194.6/66.0~~	~~30.5~~	~~53.1~~	~~52.8~~
	DM3	37.3976	27.2433	21	Plio.	marl	+	1130.0	1.004	1.037	1.045	0.794	117.0/02.3	026.3/04.0	237.4/85.4	117.0/02.3	026.8/04.0	237.4/85.4	41.5	41.5	08.0
	DM4	37.3955	27.3511	27	Plio.	lmst	+	0772.0	1.005	1.007	1.013	0.184	299.2/10.8	209.0/00.9	114.1/79.2	299.2/10.8	209.0/00.9	114.1/79.2	63.1	63.2	37.0
Plio.	**mean**			48	Plio.			0927.0	1.004	1.02	1.027	0.451	120.2/00.2	030.2/03.5	213.0/86.5	120.2/00.2	030.2/03.5	213.0/86.5	59.8	59.8	11.9
Dinar	~~BU4~~	~~38.0392~~	~~30.0896~~	~~07~~	~~Plio.~~	~~mud-marl~~	~~080/11~~	~~0050.4~~	~~1.038~~	~~1.358~~	~~1.534~~	~~0.393~~	~~306.2/61.6~~	~~207.1/04.9~~	~~114.5/27.9~~	~~287.1/68.3~~	~~027.0/03.9~~	~~118.5/21.3~~	~~20.5~~	~~20.8~~	~~08.5~~
	~~SK10~~	~~37.9578~~	~~29.8946~~	~~13~~	~~Plio.~~	~~mud-marl~~	~~215/06~~	~~0621.0~~	~~1.008~~	~~1.006~~	~~1.014~~	~~-0.142~~	~~039.0/84.8~~	~~283.9/02.2~~	~~193.8/04.7~~	~~347.6/82.4~~	~~103.9/003.4~~	~~194.3/06.8~~	~~27.8~~	~~33.2~~	~~28.6~~
Plio.	**mean**													No availble data!							
Elmalı	ST1	36.4245	29.5558	28	E.-Mid.Mio.	lmst	255/40	1020.0	1.017	1.040	1.060	0.381	296.2/21.8	042.0/34.1	180.0/47.8	120.4/06.2	029.5/08.0	248.0/79.9	31.6	33.7	18.5
	ST2	36.3789	29.5091	33	E.-Mid.Mio.	lmst	231/42	0078.0	1.007	1.018	1.026	0.390	249.6/04.5	344.2/45.4	155.3/44.2	068.0/08.9	337.1/05.6	215.4/79.4	13.1	13.0	07.4
	ST3	36.6075	29.7410	20	E.-Mid.Mio.	lmst	185/45	0305.0	1.011	1.029	1.042	0.430	348.5/16.2	240.3/47.1	091.8/38.4	342.0/00.2	252.0/07.0	073.9/83.0	22.6	22.5	10.7
	ST4	36.3795	29.9363	22	E.-Mid.Mio.	lmst	274/31	0083.7	1.005	1.018	1.025	0.580	300.4/05.0	031.8/15.5	193.1/73.7	119.5/08.8	211.4/12.1	354.2/74.9	15.7	15.7	06.5
	ST5	37.0515	30.1534	20	E.-Mid.Mio.	lmst	220/40	0044.6	1.006	1.020	1.028	0.511	025.1/25.4	284.1/22.0	158.5/55.3	012.5/10.3	105.2/14.5	248.2/72.1	20.4	20.6	12.0
	~~ST6~~	~~37.0387~~	~~30.0888~~	~~09~~	~~E.-Mid.Mio.~~	~~mud-marl~~	~~145/66~~	~~0440.0~~	~~1.029~~	~~1.053~~	~~1.084~~	~~0.292~~	~~181.7/01.8~~	~~272.3/17.1~~	~~085.8/72.8~~	~~343.7/32.2~~	~~100.0/35.1~~	~~223.9/38.3~~	~~03.3~~	~~03.7~~	~~03.7~~
	~~EL1~~	~~36.5159~~	~~29.6760~~	~~08~~	~~E.-Mid.Mio.~~	~~mud-marl~~	~~230/32~~	~~-0004.5~~	~~1.133~~	~~1.113~~	~~1.272~~	~~-0.040~~	~~059.1/05.4~~	~~151.9/27.5~~	~~318.9/61.9~~	~~054.8/09.4~~	~~160.4/58.3~~	~~319.4/29.9~~	~~73.8~~	~~73.8~~	~~58.4~~
	EL2	36.5489	29.6611	05	E.-Mid.Mio.	mud-marl	234/08	0889.0	1.033	1.053	1.089	0.228	006.1/12.1	271.9/19.2	126.4/67.0	005.3/06.1	273.7/14.2	117.8/74.5	03.4	05.2	04.2
	SK3	36.4740	29.6417	05	E.-Mid.Mio.	mud-marl	220/29	0048.0	1.011	1.015	1.027	0.132	323.8/30.6	226.1/12.8	116.2/56.2	321.9/02.3	231.6/08.3	067.4/81.4	13.3	15.2	12.8
	~~SK4~~	~~36.5369~~	~~29.7052~~	~~10~~	~~E.-Mid.Mio.~~	~~mud-marl~~	~~210/21~~	~~0000.2~~	~~1.153~~	~~1.265~~	~~1.496~~	~~-0.092~~	~~331.0/23.9~~	~~066.5/44.1~~	~~222.0/36.4~~	~~328.3/05.6~~	~~068.0/59.8~~	~~235.0/29.6~~	~~82.4~~	~~82.4~~	~~46.7~~
	GM	36.5308	29.6615	316	E.-Mid.Mio.	mud-marl	220/26	0885.0	1.021	1.030	1.053	0.114	320.0/14.2	222.5/27.3	074.5/58.6	142.5/09.5	234.2/10.0	009.8/76.2	30.7	31.2	29.0
E.-Mid. Mio.	**mean**			33	E.-Mid.Mio.			0722.0	1.018	1.028	1.049	0.214	317.5/18.7	221.7/16.7	092.8/64.5	141.7/07.2	232.4/04.9	356.1/81.3	35.8	36.2	26.5
Fethiye	~~FE1~~	~~36.7181~~	~~29.4228~~	~~09~~	~~M.Mio.~~	~~mud-marl~~	~~290/35~~	~~0539.0~~	~~1.023~~	~~1.032~~	~~1.057~~	~~0.136~~	~~015.8/02.8~~	~~284.1/32.2~~	~~110.2/57.7~~	~~195.0/32.1~~	~~305.5/29.1~~	~~067.9/43.9~~	~~25.6~~	~~25.7~~	~~13.7~~
	FE2	36.7098	29.4162	13	M.Mio.	mud-marl	321/20	0127.0	1.008	1.029	1.039	0.580	325.3/14.6	058.6/12.2	186.9/70.8	330.1/12.3	238.5/07.6	117.3/75.5	42.4	42.3	25.2
	FE4	36.4531	29.2902	12	Plio.	mud-marl	045/20	0639.0	1.007	1.012	1.019	0.276	286.1/03.2	016.2/01.0	122.8/86.6	284.0/20.6	018.0/10.4	132.2/66.7	35.8	35.9	22.1
	FE6	36.3603	29.3307	05	Plio.	mud-marl	045/20	0881.0	1.005	1.007	1.013	0.032	130.7/11.0	038.8/09.8	268.1/75.2	310.8/09.0	042.6/11.3	183.1/75.5	71.1	71.2	23.9
	SK1	36.6460	29.3980	09	M.Mio.	mud-marl	215/12	0286.0	1.016	1.042	1.061	0.438	353.9/01.4	263.3/23.5	087.0/66.4	174.3/06.5	266.0/14.4	060.6/74.2	20.8	23.7	13.7
	SK2	36.4622	29.3633	08	Plio.	mud-marl	000/10	3690.0	1.009	1.075	1.093	0.740	029.6/14.9	119.6/00.3	210.9/75.1	031.5/09.8	300.0/08.4	170.2/77.1	32.3	32.3	06.1
Plio.	**mean**			25	Plio.			1670.0	1.007	1.031	1.042	0.376	086.5/06.8	355.3/10.4	209.1/77.5	067.3/00.6	337.2/14.5	159.8/75.5	79.1	79.1	12.9
M. Mio.				22	M.Mio.			0192.0	1.011	1.034	1.048	0.522	342.7/10.9	251.3/07.2	128.6/76.9	349.9/01.2	259.6/13.5	084.7/76.5	39.3	38.2	21.1
Ören	OR1	37.1673	27.8175	14	E.-Mid. Mio.	mud-marl	089/05	0021.7	1.016	1.015	1.032	-0.082	154.7/07.9	249.8/32.7	052.8/56.1	154.9/03.3	246.9/31.0	059.3/58.8	31.9	56.8	56.8
	~~OR2~~	~~37.1533~~	~~27.8866~~	~~07~~	~~E.-Mid. Mio.~~	~~mud-marl~~	~~153/32~~	~~-0005.7~~	~~1.087~~	~~1.079~~	~~1.185~~	~~0.119~~	~~126.7/49.3~~	~~300.67/40.6~~	~~033.2/03.0~~	~~168.0/52.8~~	~~285.9/19.6~~	~~027.9/30.2~~	~~45.6~~	~~45.9~~	~~21.1~~
	~~OR3~~	~~37.0757~~	~~27.9431~~	~~08~~	~~E.-Mid. Mio.~~	~~mud-marl~~	~~344/18~~	~~-0008.8~~	~~1.041~~	~~1.075~~	~~1.123~~	~~0.294~~	~~317.2/47.7~~	~~225.6/01.5~~	~~134.3/42.3~~	~~338.3/52.8~~	~~224.2/17.2~~	~~123.1/31.8~~	~~66.7~~	~~65.6~~	~~41.7~~
	~~OR4~~	~~37.0473~~	~~28.0191~~	~~11~~	~~E.-Mid. Mio.~~	~~mud-marl~~	~~260/18~~	~~-0002.4~~	~~0.970~~	~~1.008~~	~~1.144~~	~~-0.194~~	~~006.4/20.3~~	~~100.3/17.2~~	~~230.2/62.9~~	~~005.4/03.0~~	~~096.7/23.4~~	~~268.6/66.6~~	~~18.9~~	~~23.8~~	~~25.4~~
	~~OR5~~	~~37.0582~~	~~28.1703~~	~~13~~	~~E.-Mid. Mio.~~	~~mud-marl~~	~~290/10~~	~~0074.9~~	~~1.016~~	~~1.023~~	~~1.040~~	~~0.196~~	~~215.6/06.4~~	~~123.2/20.0~~	~~322.6/68.9~~	~~216.1/16.1~~	~~119.5/22.0~~	~~339.3/62.3~~	~~12.9~~	~~14.5~~	~~13.7~~
	OR6	37.1838	27.8378	09	E.-Mid. Mio.	mud-marl	203/17	0620.0	1.003	1.003	1.006	0.110	295.6/03.1	205.4/05.0	057.6/84.2	115.7/13.9	206.7/04.0	312.6/75.5	43.5	44.9	36.5
	~~YT1~~	~~37.2353~~	~~28.1945~~	~~04~~	~~E.-Mid. Mio.~~	~~mud-marl~~	~~075/11~~								No available data!						
	~~YT2~~	~~37.2632~~	~~28.1083~~	~~02~~	~~E.-Mid. Mio.~~	~~mud-marl~~	~~000/12~~								No available data!						
	YT3	37.3641	28.0549	11	E.-Mid. Mio.	mud-marl	305/08	0030.3	1.024	1.069	1.100	0.492	310.9/07.6	041.2/02.3	147.9/82.1	311.9/06.7	221.3/05.7	091.2/81.2	55.1	55.1	08.3
E.-Mid. Mio.	**mean**			29	E.-Mid. Mio.			0211.0	1.016	1.030	1.049	0.128	319.7/05.2	049.7/00.1	141.3/84.8	322.1/03.9	231.7/06.0	085.1/82.9	57.2	57.2	11.7
Tavas	TVS1	37.6254	29.0066	32	Lt. Mio.	mud-marl	+	1650.0	1.003	1.006	1.009	0.370	158.5/02.1	248.5/00.6	355.4/87.8	158.5/02.1	248.5/00.6	355.4/87.8	77.0	77.0	18.4
	TVS2	37.5142	28.8237	28	Lt. Mio.	mud-marl	203/31	1690.0	1.010	1.027	1.039	0.425	287.3/16.2	193.4/13.2	066.2/68.9	107.4/14.6	201.7/16.2	337.4/67.9	15.7	16.0	09.9
	TVS3	37.5581	28.7865	22	Lt. Mio.	mud-marl	+	1230.0	1.001	1.002	1.003	0.090	067.7/07.4	337.2/03.9	219.5/81.6	067.7/07.4	337.2/03.9	219.5/81.6	60.2	60.2	34.9
	~~TVS4~~	~~37.5345~~	~~28.6366~~	~~20~~	~~Lt. Mio.~~	~~mud-marl~~	~~+~~	~~0002.9~~	~~3.040~~	~~1.111~~	~~1.332~~	~~0.192~~	~~172.4/76.3~~	~~285.1/05.4~~	~~016.3/12.6~~	~~172.4/76.3~~	~~285.1/05.4~~	~~016.3/12.6~~	~~27.0~~	~~36.4~~	~~31.4~~
	TVS5	37.4681	28.6498	16	Lt. Mio.	lmst	142/06	0095.7	1.012	1.042	1.057	0.560	330.0/14.1	060.5/02.2	159.3/75.7	328.4/14.9	060.6/08.2	178.5/73.0	58.9	58.8	10.7
	KL1	37.2711	28.6523	12	Ol.-E.Mio.	mud-marl	158/26	0341.0	1.005	1.019	1.025	0.569	171.6/40.4	078.9/03.2	345.1/49.4	189.0/30.3	080.4/28.7	316.0/45.8	06.4	06.4	03.0
	KL2	37.2707	28.6187	17	Ol.-E.Mio.	mud-marl	044/55	1110.0	1.007	1.092	1.112	0.853	206.8/32.4	078.1/44.6	316.5/28.0	188.2/05.9	097.7/04.3	331.7/82.7	56.1	56.0	10.1
	KL3	37.2773	28.6246	29	E.Mio.	mud-marl	056/34	2260.0	1.004	1.052	1.063	0.858	210.1/30.6	099.4/31.0	334.5/43.6	198.4/12.2	107.2/05.6	353.2/76.5	26.5	26.6	06.2
	KL4	37.3237	28.6275	21	Ol.-E.Mio.	mud-marl	310/26	1210.0	1.023	1.077	1.107	0.522	343.2/05.6	076.1/27.4	242.62/61.9	162.6/08.7	308.8/79.6	308.8/79.6	05.5	05.5	03.7
	KL5	37.3719	28.5949	20	E.Mio.	mud-marl	214/11	0647.0	1.004	1.021	1.027	0.698	187.3/05.5	097.1/01.3	353.6/84.3	188.7/10.4	096.6/11.1	320.6/74.7	69.9	69.9	09.1
	~~KL6~~	~~37.3673~~	~~28.6562~~	~~16~~	~~E.Mio.~~	~~mud-marl~~	~~202/11~~	~~0011.1~~	~~1.071~~	~~1.103~~	~~1.192~~	~~0.305~~	~~328.7/08.1~~	~~237.2/10.6~~	~~095.3/76.6~~	~~328.7/08.1~~	~~238.3/04.2~~	~~048.1/85.8~~	~~54.9~~	~~54.8~~	~~24.2~~
Lt. Mio.	**mean**			98	Lt. Mio.			1310.0	1.006	1.017	1.024	0.354	295.4/11.4	204.8/02.9	100.6/78.2	100.1/05.3	190.2/01.1	292.1/84.5	37.5	37.8	31.3
Ol.-E. Mio.				99	Ol.-E.Mio.			1280.0	1.009	1.054	1.069	0.719	059.9/13.8	158.4/31.0	309.0/55.4	173.5/10.5	082.7/04.5	329.6/78.6	30.3	30.3	8.5
Ulubey	~~PK1~~	~~38.0081~~	~~29.1435~~	~~12~~	~~Plio.~~	~~sand-marl~~	~~304/09~~	~~0021.8~~	~~1.028~~	~~1.022~~	~~1.052~~	~~-0.040~~	~~333.0/13.6~~	~~065.5/10.2~~	~~191.3/72.9~~	~~333.0/13.6~~	~~065.0/02.5~~	~~170.3/80.6~~	~~52.1~~	~~50.8~~	~~41.8~~
	CL1	37.8167	29.2797	14	Plio.	mud-marl	136/16	0414.0	1.010	1.026	1.038	0.415	194.7/08.3	285.5/05.8	050.1/79.8	014.9/5.4	105.1/02.4	218.9/84.1	23.1	23.2	9.6
	~~CL2~~	~~38.3445~~	~~29.5783~~	~~13~~	~~Plio.~~	~~mud-marl~~	~~+~~	~~0023.1~~	~~1.016~~	~~1.018~~	~~1.036~~	~~0.035~~	~~309.5/70.1~~	~~177.4/13.6~~	~~83.9 /14.2~~	~~309.5/70.1~~	~~177.4/13.6~~	~~83.9 /14.2~~	~~51.9~~	~~58.6~~	~~57.5~~
	CL3	38.5414	29.6563	15	Plio.	lmst	057/08	2280.0	1.006	1.022	1.029	0.477	053.7/01.2	143.8/07.2	314.5/82.7	053.9/1.6	323.9/00.8	206.6/88.2	37.3	37.2	14.6
	~~UL1~~	~~38.3454~~	~~29.2171~~	~~12~~	Plio.	marl	~~+~~	~~0009.1~~	~~1.100~~	~~1.145~~	~~1.291~~	~~-0.111~~	~~117.0/11.5~~	~~359.6/66.2~~	~~211.4/20.5~~	~~117.0/11.5~~	~~359.6/66.2~~	~~211.4/20.5~~	~~46.5~~	~~62.6~~	~~62.2~~
	~~UL2~~	~~38.4193~~	~~29.2599~~	~~8~~	~~Plio.~~	~~marl~~	~~+~~	~~0004.7~~	~~1.055~~	~~1.076~~	~~1.142~~	~~0.010~~	~~75.00/37.1~~	~~187.6/26.9~~	~~303.8/41.1~~	~~75.00/37.1~~	~~187.6/26.9~~	~~303.8/41.1~~	~~47.9~~	~~47.9~~	~~45.1~~
	UL4	38.3245	29.1011	15	Plio.	mud-marl	+	2090.0	1.005	1.035	1.044	0.576	222.3/04.1	132.0/05.3	349.9/83.2	222.3/4.1	132.0/05.3	349.9/83.2	25.7	25.7	7.3
	~~UL5~~	~~38.1230~~	~~29.0384~~	~~15~~	~~Plio.~~	~~sand-marl~~	~~136 / 10~~	~~0009.2~~	~~1.070~~	~~1.054~~	~~1.139~~	~~0.111~~	~~280.0/16.9~~	~~182.7/22.7~~	~~043.4/61.6~~	~~278.0/10.9~~	~~185.0/15.3~~	~~042.1/71.1~~	~~28.8~~	~~19.9~~	~~30.5~~
	UL6	38.0457	28.9604	13	Plio.	sand-marl	+	1800.0	1.003	1.003	1.006	-0.057	160.2/22.0	307.9/64.5	065.1/12.3	160.2/22.0	307.9/64.5	065.1/12.3	39	39.1	17.3
Plio.	**mean**			57	Plio.			1660.0	1.006	1.022	1.028	0.366	198.4/06.5	108.3/01.4	006.1/83.3	200.2/00.3	110.2/01.9	300.3/88.1	46.6	46.6	11.5
											REGIONAL										
Lt. Mio.-Plio.	**mean**			784	Lt. Mio.-Plio.			0612.0	1.006	1.018	1.024	0.382	069.5/02.1	159.6/01.7	288.2/87.3	072.6/00.6	342.5/01.2	187.5/88.6	72.0	72.0	18.0
Ol.-Mid. Mio.	**mean**			599	Ol.-M. Mio.			0771.0	1.016	1.033	1.050	0.305	325.2/09.2	233.2/12.1	091.5/74.7	145.9/07.4	236.4/03.6	352.2/81.7	40.0	40.1	20.7

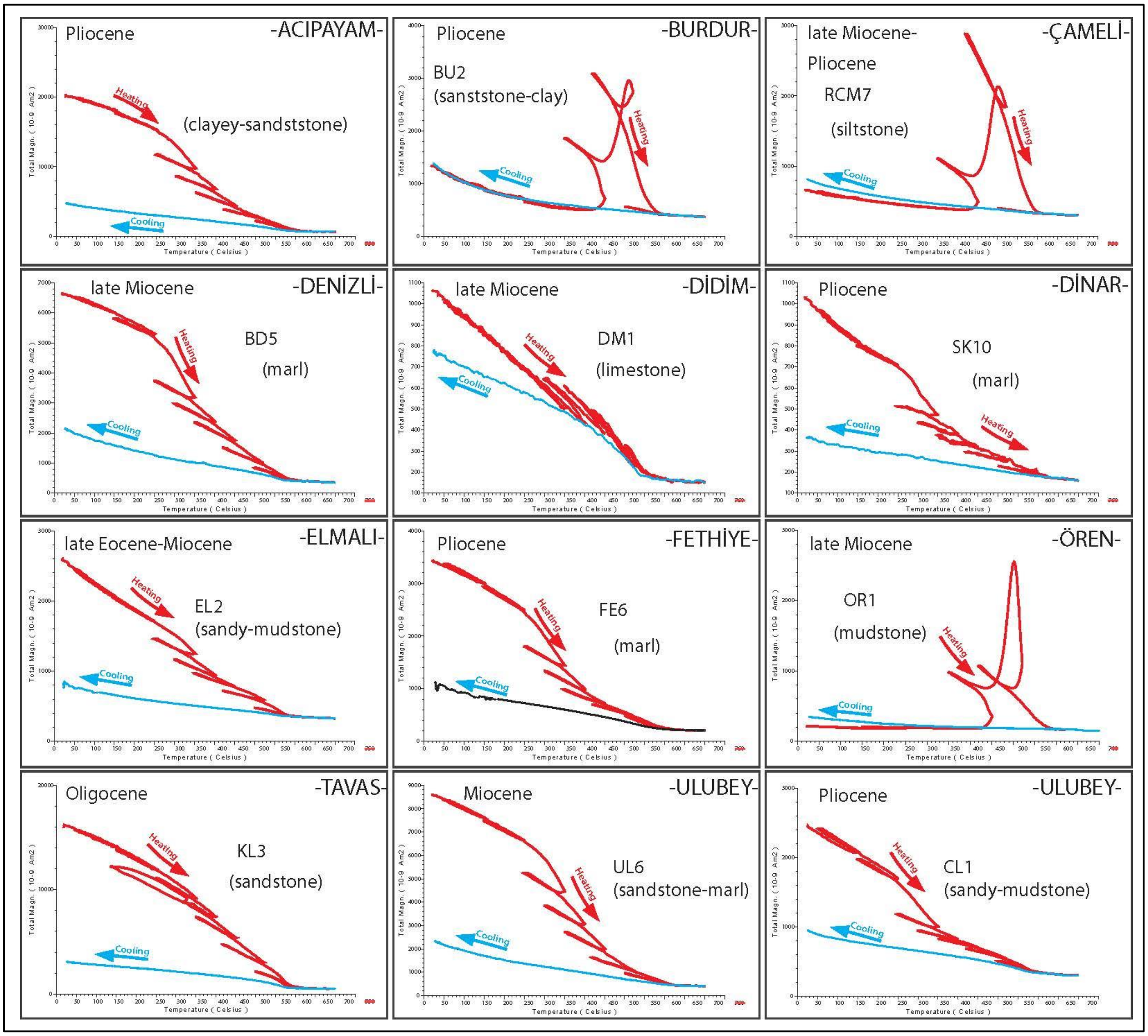

Figure 2. Representative thermomagnetic curves for each site, consisting of several heating-cooling cycles to asses changes (alterations) in the magnetic properties (Mullender et al., 1993). The final cooling curve is indicated with the blue line. See the text for an explanation of the thermomagnetic behavior.

3.2. Origin of anisotropy of magnetic susceptibility

The site mean AMS parameters after tilt correction of 83 sites, and their location means are listed in Table 1. Figures of the results per site are given in Figure 4. To illustrate the rock magnetic mineral properties of all analyzed sites, we plot the mean susceptibility values (k_m) of all specimens from both Miocene and Pliocene sedimentary rocks (Figure 3). The k_m values show a wide range, from very low and even negative (diamagnetism), from -10 up to very high values of more than 6000 x 10^{-6} SI. There are two main clusters, one around 25-75 x 10^{-6} and one around 1000-5000x10^{-6} SI (Figure 3a and Table 1). When the Miocene and Pliocene samples are compared, especially the Miocene specimens exhibit the highest susceptibilities and dominate the high susceptibility cluster, which is consistent with the petrographic point of in which Miocene samples are obtained dominantly of fine clastic material such as mudstones while Late Miocene-Pliocene samples collected dominantly from marl and limestones. The k_m values show a wide range proving that the specimens include a varying composition and concentration of (ferro-) magnetic minerals. In other words, the k_m distribution is partly dependent on the age of the specimens (Lower-Middle Miocene samples have larger values) but partly varies depending on the magneto-mineral composition. Distributions of the maximum (k_1), intermediate (k_2), and minimum (k_3) susceptibility axes at the site level also exhibit a variable degree of clustering, from quite scattered (large confidence ellipses) to very well-defined clusters (Table 1). The sites with statistically insufficient sampling numbers and showing considerable scatter in the three susceptibility axes (confidence ellipses >50°) were excluded from further analysis. The discarded site mean results are given in Table 1, and accepted sites are shown in Figure 4. Most of the rejected sites (24) have very low to negative susceptibilities (diamagnetic) and cannot be used. Mixed magnetic mineral content and/or secondary magnetization effects may also adversely influence the magnetic fabric (Rochette, 1987; Rochette et al., 1992).

The distributions of the susceptibility axes directions after tilt correction from the remaining number of accepted (59) sites that meet the criteria generally present a predominantly oblate shape, which reflects the essentially sedimentary origin of the fabric (k_3 typically vertical and perpendicular to the bedding plane). However, the clustering of the k_1 and k_2 axes reflect the type and magnitude of the tectonic deformation prevailing in the region. The mean foliation parameters (F) have small scattering between $1.002 \leq F \leq 1.358$ ($F_{mean} = 1.04$). Site mean magnetic lineation (L) parameters range between $0.970 \leq L \leq 3.040$ ($L_{mean} = 1.046$). Although L_{mean} is slightly higher than F_{mean} – due to particularly high lineation values from site TVS4 (rejected from further analyses, Table 1) – it is clear from Figure 3b that the large majority of the foliation values is higher than the lineation values, reflecting the mainly oblate character of the distributions, in particular for the range with both L and F less than 1.2. The corrected anisotropy degree Pj is in general relatively low with a dominant mean clustering around Pj = 1.02, although the arithmetic mean ($P_{jmean} = 1.073$) is quite high, due to sites with very high values, up to a maximum of $P_j = 1.534$ (e.g., site BU4, Table 1). In general, the shape of the AMS ellipsoids are mostly moderately oblate (Figure 3c), but also negative T values(prolate) occur. We note that there is no evident correlation between T and Pj, indicating there is no correlation with, for example, lithological variations or the temporal-spatial distribution of the sites, suggesting that strain essentially determines the AMS (Figure 3c).

3.3. AMS results

The equal-area projections of the AMS ellipsoids from each of the 60 sampled sites after bedding plane correction are illustrated in Figure 4. A total of 24 sites that failed to meet the criteria for the reasons described above were excluded from the database (Figure 4, Table 1). Subsequently, the obtained site-based orientation of the AMS ellipsoid results was combined into the 11 different domains according to their geologic and geographic positions. The obtained results are compared with the previously mapped normal faults (Kaymakcı et al., 2018) in each domain. Domain-based combined results depicted in Figure 5.

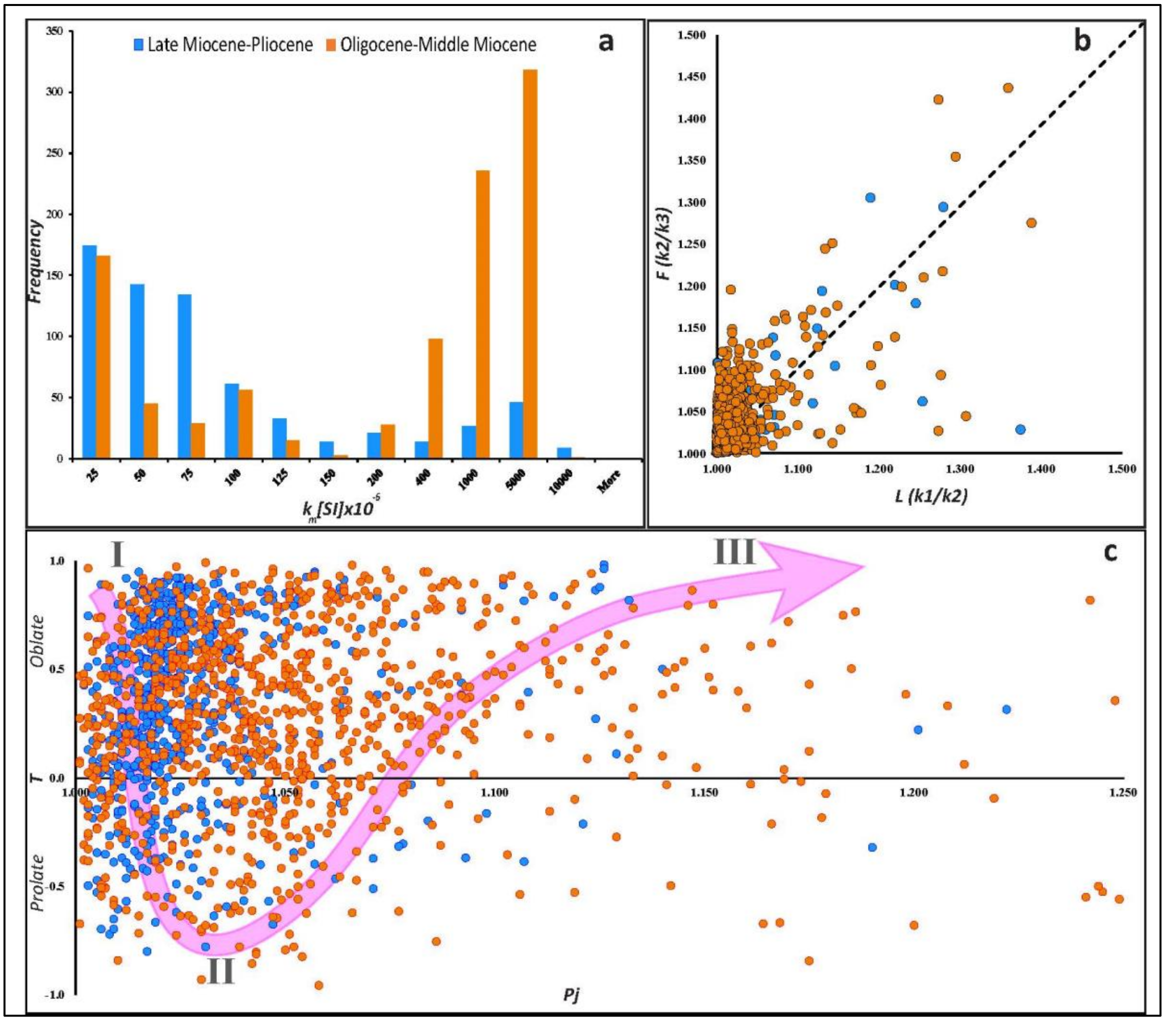

Figure 3. a) Frequency distribution of the magnetic susceptibility (km) from all measured specimens. b) Anisotropy plots of magnetic foliation (F) versus magnetic lineation ratios (L). c) Shape factor (T) versus corrected anisotropy degree (Pj) diagram compared to the typical trend expected from an increasing degree of deformation, from an oblate sedimentary magnetic fabric (I) to a prolate tectonic-sedimentary fabric (II) and finally to an oblate purely tectonic fabric.

3.3.1. Acıpayam Domain

In the Acıpayam Domain, five sites in Pliocene mudstones and limestones lithologies are sampled. The limestone site (PK2) has very low magnetic intensity and a very large confidence ellipse. Therefore, it is disregarded for further analysis (Table 1). The remaining Late Miocene (PK3 and PK4) and Pliocene sites (EL3 and EL4) indicate NNE-SSW to NE-SW orientations of maximum anisotropy axes (lineations). The normal faults in the Acıpayam domain are striking NE-SW and NW-SE (Figure 4). The lineations in the sites EL3, EL4, and PK3 are almost perpendicular to NW-SE striking nearby normal faults. Whereas the site PK4 is parallel to the strikes of the nearby normal faults, which is, in fact, perpendicular to NW-SE striking main boundary faults of the Acıpayam Basin (Figure 4). The combination of the accepted four sites includes 33 specimens, and they altogether indicate NE-SW (237˚N) oriented magnetic lineation after tilt correction, which is almost the same as the in situ orientation (239˚N) (Figure 5, Table

1). The discrepancy between the trend of the mean maximum anisotropy direction and the strike of the bedding is around 27˚, implying that they are oblique to each other.

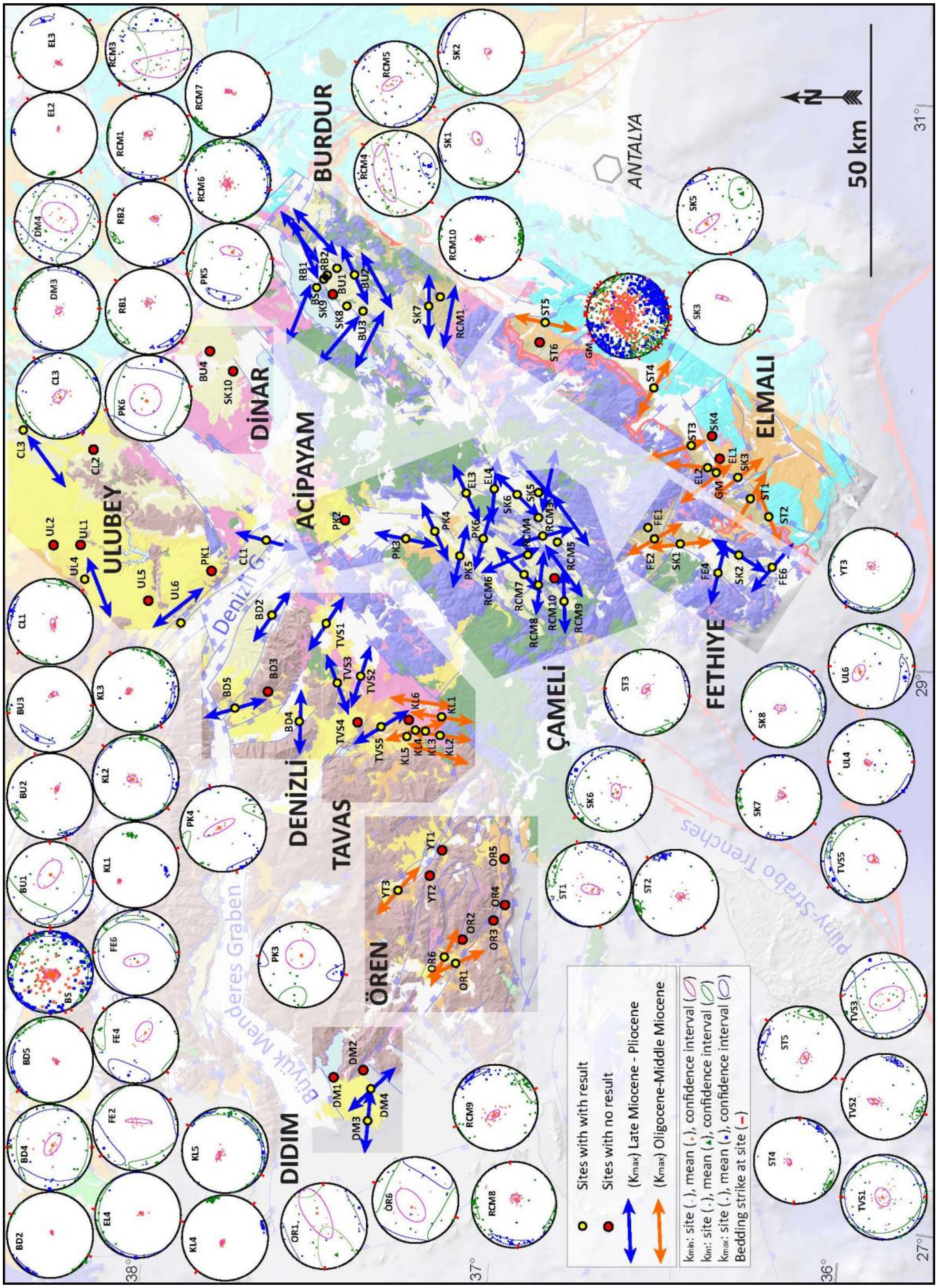

Figure 4. The orientations of site mean magnetic lineations (k_{max}) after bedding plane correction per site.

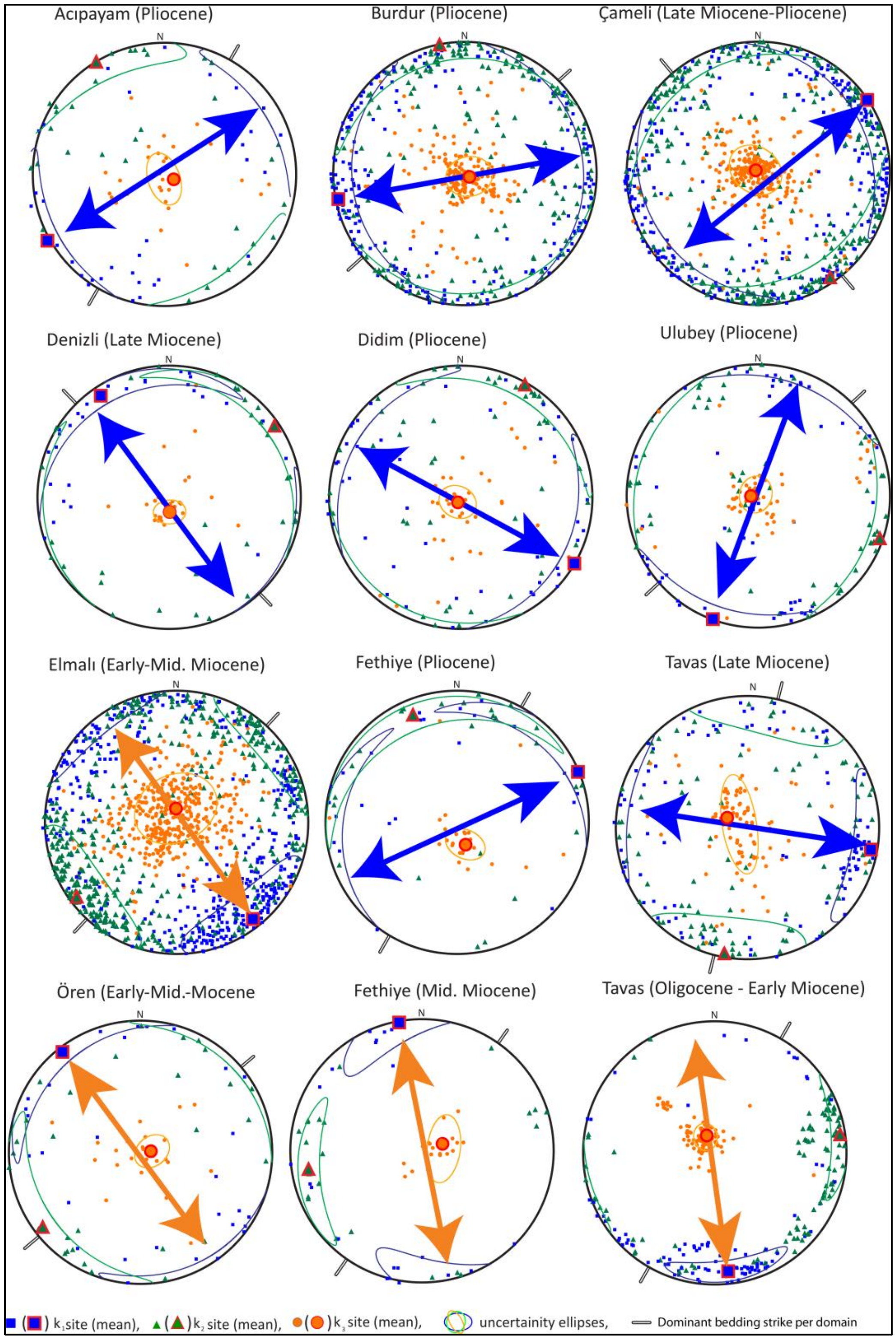

Figure 5. Lower hemisphere equal area plots of the three axes of the anisotropy of the magnetic susceptibility ellipsoids from the 11 domains after bedding plane correction. The site-based AMS results are given in Table 1.

3.3.2. Burdur Domain

The Burdur Domain is based on ten sites (Figure 4) collected from Pliocene sandstone-claystone and marl-mudstone in the easternmost part of the study area (Figure 1). The ten sites have a low to moderate mean magnetic susceptibility results, and values change between 6.7 and 174x10^{-6} (SI) (Table 1). Site SK9 provided scattered AMS directions, and low magnetic susceptibility (6.71x10^{-6}) was discarded (Table 1). The site BS belongs to a magnetostratigraphic sampling site (Özkaptan et al., 2018). Therefore, it contains a very large data set and indicate NW-SE oriented lineation, different from the nearby sites.
The results show that K_{max} lineations are oriented dominantly in two directions. The sites BS, SK8, BU3, and RCM1 are oriented NW-SE while the sites SK7, BU2, BU1, RB2, and RB1 oriented NE-SW (Figure 4, Table 1) The combination of all sites (197 specimens) produced k_{max} oriented in 084˚N in situ and 259˚N after bedding correction. The lineations are generally parallel to the local bedding strikes. The dominant strikes of the normal faults in the Burdur domain are oriented NE-SW almost perpendicular to the obtained mean lineation direction (Figure 4). The discrepancy between the trend of the mean maximum anisotropy direction and the strike of the bedding is around 36˚, implying that they are oblique to each other.

3.3.3. Çameli Domain

The Çameli Domain consists of 12 sites; eight sites are collected from Late Miocene-Pliocene marl, sandstone, mudstone intercalations, and four sites from Pliocene claystone (Table 1). Two sites (RCM3 and RECM4) have very low mean magnetic susceptibility values of ~10x10^{-6} (SI) and larger confidence ellipses than the other sites in the area. However, their AMS directions are consistent and not scattered very much. Therefore, they all are used for further analysis. The remaining ten sites have at least ~50x10^{-6} (SI) mean magnetic susceptibility values, but one site (PK5) has extremely high mean magnetic susceptibility values reaching up to 2320x10^{-6} (SI) (Table 1).
Similar to the Burdur domain, the lineations in the Çameli domain are also oriented in two dominant directions. The first group includes the sites RCM3, RMC4, RMC6, RCM8, PK5, PK6 and are oriented, in general, NW-SE. In the remain sites, the k_{max} is generally oriented in NE-SW (Figure 4). Since there is no age or tectonic setting difference between the sites, these two dominant directions are interpreted as the result of the multi-directional extension. In addition, the AMS results in all sites do not show any significant discrepancy in both in-situ and tilt corrected coordinates (Table 1, Figures 4, 5) due to their orthogonal nature with respect to bedding attitudes, in other words, the bedding plane strikes are almost perpendicular or parallel to one of the princğpal AMS directions, except for site RCM5.
The combined analysis of all sites indicates that k_{max} is oriented NE-SW while k_{int} is oriented NW-SE. The discrepancy between the trend of the mean maximum anisotropy direction (048˚ in situ and 056˚N after tilt correction) and the strike of the bedding (320˚N) is around 88˚-96˚.

3.3.4. Denizli Domain

In the Denizli, Domain comprises four Late Miocene-Pliocene sites (BD2, BD3, BD4, BD5) composed of clayey-limestone and marls. The limestone sample (BD3) produced scattered directions with a very large confidence interval (>50°) for all three AMS axes. Therefore it is discarded and not used for further analysis (Table 1). The combined analysis of marl bearing sites, BD2 and BD5, indicate ~NW-SE trending lineations, while in site BD4 – also sampled in horizontal marl layers – produced almost E-W lineation. Strikes of the local bedding planes of BD2 and BD5 are perpendicular to the direction of the magnetic lineations. A combination of all sites (31 specimens) indicates AMS lineation of NW-SE (331˚N in situ and 326°N after tilt correction) (Figure 5). This orientation is almost parallel to the dominant trends of the normal faults in the domain (Figure 6), while the discrepancy between the trend of the mean maximum anisotropy direction and the dominant bedding strike (136N) for the domain is around 10˚-15˚ (Table 1) implying that they are almost parallel.

3.3.5. Didim Domain

The Didim Domain contains four sites sampled in Pliocene limestones and marls. The limestone sites (DM1 and DM2) were discarded due to low mean magnetic susceptibility and large scattered AMS directions. The remaining sites, DM3 and DM4, have a moderate to high mean magnetic susceptibility of 1130 and 772x10-6 (SI), respectively. On the site basis, the lineation in both sites is oriented about NW-SE. A combination of these two sites produced from 48 specimens mean AMS lineation of ~NW-SE (120°) (Table 1, Figure 5). The Didim domain is almost undeformed, and reliable sites are almost horizontal. However, there are some normal faults developed at the margin of the domain, and the mean lineation direction is perpendicular to the normal faults around the domain (Figure 6).

3.3.6. Dinar Domain

From the Dinar Domain in the north-eastern part of the study area (Figure 1), only two sites were sampled, both comprise in Pliocene limestone and marl units. The mean magnetic susceptibility in both sites is low to moderate, ranging between 50 and 620 x 10^{-6} (SI) (Table 1). However, the results are scattered, and both sites have very high confidence intervals (>50˚); therefore, they are disregarded from further analysis (Table 1).

3.3.7. Elmalı Domain

The Elmalı Domain was sampled at eleven sites in Early-Middle Miocene sandstone-mudstone-claystone and limestone units. Two limestone sites (EL1 and SK4) yielded erratic directions, and almost zero mean magnetic susceptibility (0 to 4 x10^{-6} (SI) possibly due to diamagnetic mineral content in the matrix, hence these sites are discarded (Table 1). Despite high magnetic intensity (440x10^{-6} SI), site ST6 presents a triaxial cluster and mean k_{min} directions not normal to the bedding plane (38.3°). On the other site, the k_m values range between 44 x10^{-6} up to 1020 x10^{-6} (SI). The sites ST1, GM are sampled in sandstone-mudstone alternations and have high (para-, ferro-) magnetic mineral content. Although the bedding attitudes vary widely in each location in the domain, the lineations are generally almost parallel to bedding strikes for each site except for site SK3 (Table 1). NW-SE striking normal faults and NE-SW striking thrust faults dominate the domain. The AMS lineations are sub-perpendicular to the bedding strikes and clearly show two directions. The sites EL2, ST2, and ST5 are oriented NE-SW while the remaining sites are oriented NW-SE. Combined analysis of all sites indicates mean AMS lineation of NW-SE (317˚N Insitu, 141˚N after bedding tilt correction) direction. The discrepancy between the trend of the mean maximum anisotropy direction and the dominant strike of the bedding for the domain is around 85˚. This means that they are almost perpendicular to each other.

3.3.8. Fethiye Domain

The Fethiye domain is dominated by various normal faults developed due to ongoing extensional deformation in the region (ten Veen, 2004). Length weighted rose diagrams of the normal faults in the domain indicate two sets of dominant directions oriented NE-SW and NW-SE (Figure 6). The Fethiye domain contains six Middle Miocene to Pliocene sites composed of sandstone, mudstone, and marls. All sampled lithologies show moderate to high magnetic intensity, especially in the marl samples of site SK2, which reaches up to $3690x10^{-6}$ (SI) (Table 1). Thermomagnetic experiments also indicate that the ferromagnetic (Ti-magnetite) composition is dominant in the region (Figure 2). Despite high magnetic susceptibility and small confidence ellipses in all three axes, site FE 1 is disregarded due to the mean k3 axis not being normal (43.9°) to the bedding plane (Table 1, Figure 4). Except for site FE2, AMS lineations are almost perpendicular to bedding strikes. The Middle Miocene and Pliocene sites are combined separately to reconstruct mean AMS directions for the domain. Combination of the Pliocene sites indicates almost E-W (087˚N in situ and 067˚N after bedding tilt correction) k_{max} orientation while Middle Miocene sites indicate NNW-SSE (343˚N in situ and 350˚N after bedding tilt correction) orientation (Table 1). These two directions are almost perpendicular (80˚ in situ and 77˚ after bedding tilt correction) to each other.

The discrepancy between the in situ trend of the mean maximum anisotropy direction and the dominant strike of the bedding for the Middle Miocene units is 42˚ while it is 67˚ for Pliocene units, implying that they are diagonal to oblique to each other.

3.3.9. Ören Domain

The Ören Domain is dominated by approximately N-SE striking normal faults (Figure 4). From this domain, nine Early-Middle Miocene sites composed of mudstone, sandstone, and marls are sampled. Among these, six sites were discarded since they did not result in any reliable directions and are scattered randomly, possibly due to low magnetic susceptibility or magnetic fabric that has not recorded tectonic deformation. In addition, the YT1 and YT2 sites did not have a sufficient amount of measurements for Jelinek statistics, due to unconsolidated material broken into pieces during the transport.

The remaining sites produced interpretable results. Among them, the AMS lineations obtained from two sites (OR1, OR6) are perpendicular to the local bedding strikes while they are parallel to the bedding strikes in the site YT3. A combination of all three sites (29 specimens) shows that the mean lineation has is oriented in NW-SE (320°N, Table 1) direction. (Figure 5).

The discrepancy between the trend of the mean maximum anisotropy direction and the strike of the bedding is 90˚; in other words, they are perpendicular to each other.

3.3.10. Tavas Domain

The Tavas Domain contains eleven sites sampled in Oligocene to Late Miocene sandstone-mudstone alternations. Site TVS4 has very low (diamagnetic) mean magnetic susceptibility $2.9x10^{-6}$ (SI), and maximum susceptibility directions are clustered nearly perpendicular to the bedding plane (Tabel 1), while site KL6 has very large confidence ellipse. Therefore both sites are discarded for further analysis (Table 1). The remaining nine sites show very consistent results with a slight discrepancy between the lineations before and after tilt correction (Figure 4). The lineations in the dipping sites are generally sub-parallel to the bedding strikes except for site TVS2, where the lineation is perpendicular to the local bedding strike (Tabel 1).

The sites in the Tavas domain are grouped into two as Oligocene-Middle Miocene sites (KL1-KL5) and Late Miocene sites (TVS1-TVS5). The combined analysis of these sites indicates that the mean AMS lineament is oriented NE-SW (060˚N in situ and 174˚N after bedding tilt correction) while the mean AMS lineation for the Late Miocene sites oriented (295˚N in situ and 101˚N after bedding tilt correction) (Table 1).
The length weighted rose diagrams of normal faults developed in the domain indicate that two almost orthogonal dominant sets of normal faults are developed (Figure 6). The AMS lineations from the Oligocene-Middle Miocene and Late Miocene rocks are oriented parallel (or perpendicular) to these two dominant fault orientations (Figure 6).
The discrepancy between the trend of the in situ mean maximum anisotropy direction and the strike of the bedding for Late Miocene units is 79˚; in other words, they are orthogonal. However, it is 30˚ for the Oligocene-Middle Miocene units, indicating that they are oblique to each other.

3.3.11. Ulubey Domain

The Ulubey domain comprises nine sites composed of Pliocene limestones, sandstone, mudstone, and marl units cropping out in the northernmost part of the study area (Figure 1). Among these sites, five of them were discarded since they produced very erratic directions, with poorly clustered and low mean magnetic susceptibility values (Table 1). The remaining four sites have moderate to high magnetic susceptibility values, and in some sites, k_m reaches up to $2200x10^{-6}$ (SI), implying a ferromagnetic mineral dominant composition, which is also evident from the thermomagnetic curves (Figure 2).

Among the four sites, three of the AMS lineations are oriented NE-SW, while only the UL6 is oriented NW-SE. Combined analysis of all sites indicates NNE-SSW (198˚N in situ and 200˚N after bedding tilt correction) orientation of the mean AMS lineation (k_{max}).

Most of the sites are undeformed, and no major tectonic activity could be observed in the Ulubey domain. However, the southern and eastern margin of the domain is delimited by normal faults of the Denizli and Baklan grabens, the eastern continuation of the Büyük Menderes Graben (Figure 1). Bedding attitudes are mostly horizontal, or they are slightly tilted. Length weighted rose diagrams prepared from margin bounding normal faults dominantly oriented NW-SE (Figure 5). The mean AMA lineation direction is almost perpendicular to the dominant strikes of the normal faults and almost parallel to the dominant strike of the bedding planes (Table 1, Figure 6).

4 Discussion

4.1. Interpretation of results

In addition to the spatial differences, there are also variations in the values of magnetic susceptibility values, which can be seen as (a) a cluster of low values around 50×10^{-6} SI and (b) a cluster of high value around 5000×10^{-6} SI. The low and high values are probably associated with the dominances of (a) diamagnetic/paramagnetic or (b) ferromagnetic minerals in the samples, respectively (Figure 3a). According to previous studies, the dominance of either the paramagnetic and ferromagnetic minerals in a rock volume does not affect the AMS-patterns (e.g., Borradaile & Jackson, 2010). Especially, paramagnetic phyllosilicate (clay) minerals are highly sensitive in terms of strain indicator, more than classical strain analyses methods in weakly deformed areas (Scheepers & Langereis, 1994).

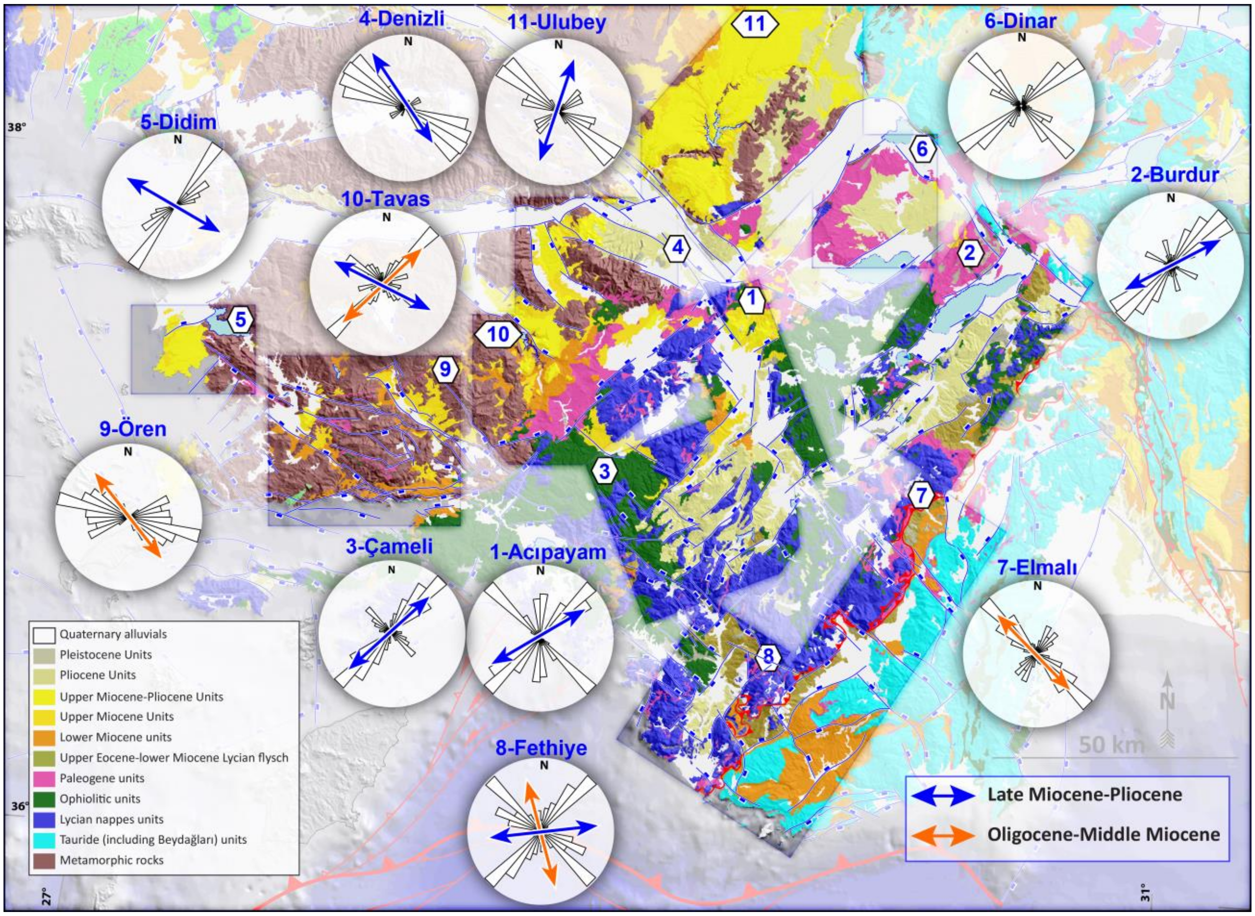

Figure 6. The orientation of the mean magnetic lineation (k_{max}) of each 11 domains after tectonic correction overlaid on length weighted rose diagrams prepared from normal faults for each domain.

In ideal conditions, such as low energy, vertical (no flow involvement), and fine-grained deposition, presence of suitable magnetic minerals, no diagenetic or other post-depositional petrographic changes, the maximum anisotropy axis (k_{max}) aligns along the maximum stretching direction in accordance with the tectonic regime (extensional or contractional) under which the sediments are deposited, even in an area where there is no clear visible evidence about the style of the deformation on the surface (e.g., Gong et al., 2009; Maffione et al., 2015; Mattei et al., 1997; Scheepers & Langereis, 1994; Soto et al., 2009). In this study, the magnetic fabric orientations in the Neogene deposits cover one of the most tectonically active extensional deformation dominated regions in the eastern Mediterranean and are used to decipher past and recent deformations. The configuration of the anisotropy directions determines the shape of the AMS tensor and provides information about the intensity and style of the deformation of the host rocks (e.g., Parés et al., 1999). The AMS shape parameter (T) versus corrected anisotropy degree (Pj) diagram (Figure 3c) indicate that most of the measurements give positive T values (clustered in the oblate region) and suggest a considerable amount of compaction related shortening (e.g., Tarling & Hrouda, 1993). However, systematic clustering of maximum (k_{max}) and intermediate

(k_{int}) anisotropy axes in the horizontal plane suggests that primary sedimentary fabric is deformed into a tectono-sedimentary fabric which facilitates determination and quantification of strain axes in space and time.

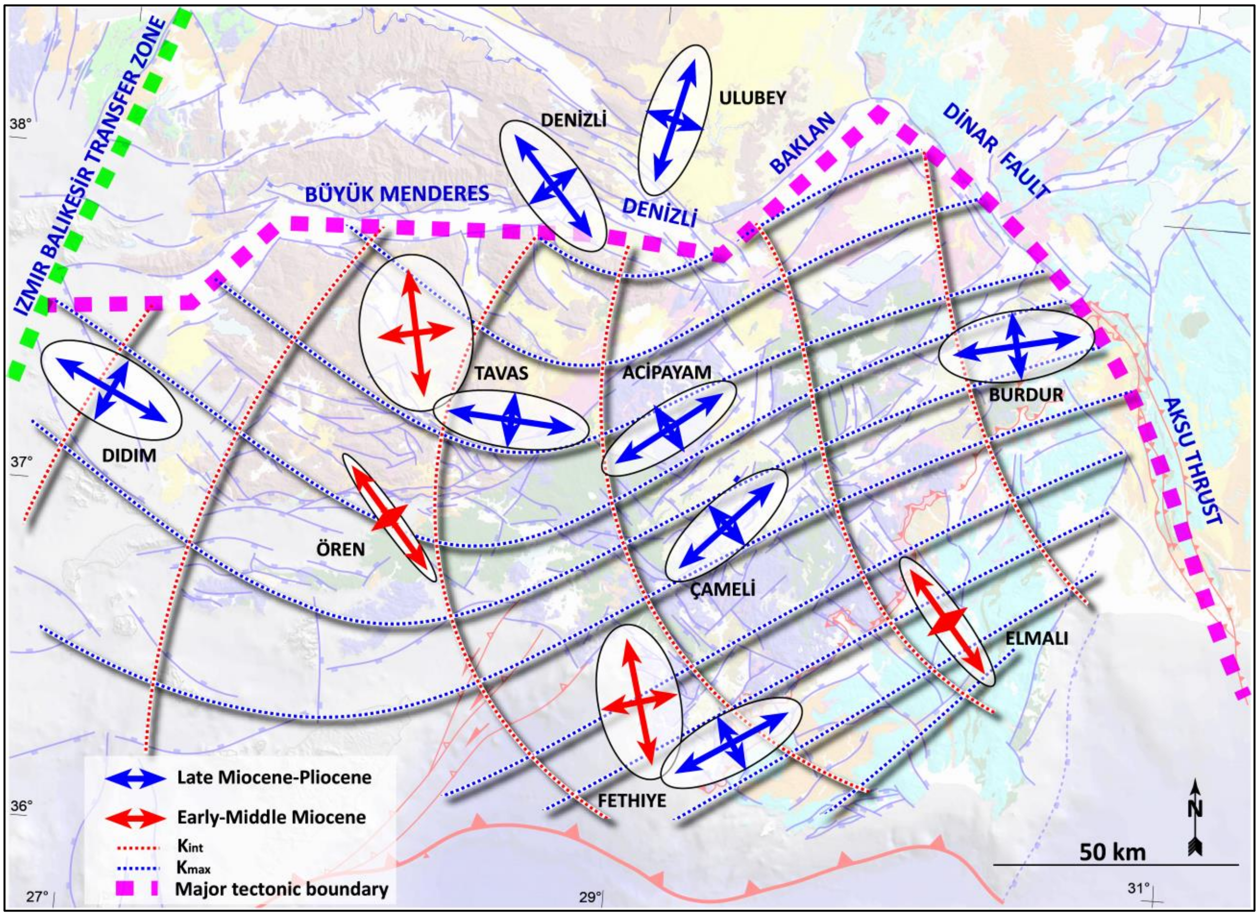

Figure 7. Strain ellipses based on directions and relative magnitudes of K_{max} and K_{int} for each domain. Dashed lines are manually constructed smoothed strain trajectories. Note near-identical geometries of Late Miocene-Pliocene strain ellipses and their variations in the Early-Middle Miocene rocks.

The AMS analyses of this study conducted on Oligocene to Pliocene sedimentary sequences of entire SW Anatolia (from 83 sites in 11 domains). Except for locations with diamagnetic susceptibilities or adverse magnetic properties, the AMS distributions show that the magnetic fabrics of the detrital sediments result from tectonic deformation. These deformation related AMS patterns are marked by well-defined bedding normal and parallel orientations and distinct magnetic lineation with low error ellipsoids (Table 1, Figure 4). The developed magnetic fabrics controlled by the geographic and geologic positions of the sites (Figure 4). The result shows that the tectonic fabrics of the Neogene deposits based on the magnetic rock analyses and AMS diagrams indicate an apparent tectonic overprint except for few rejected sites. It is unequivocally accepted that there is a major tectonic reorganization in the eastern Mediterranean region by the beginning of Late Miocene, the so-called Neotectonic period due to the collision of the Eurasian and Arabian Plates which led to the inception of the North Anatolian Fault Zone that facilitated westwards flee of the Anatolian Block (Şengör et al., 2005). Therefore, the AMS results for the Late Miocene to Pliocene are separated from the older time units.

As seen in Figure 4. The main magnetic lineament directions are either parallel (mostly) or almost perpendicular to nearby faults, except for one site in Didim, and almost all of the Oligocene-Middle Miocene sites in Tavas basins, which are oblique to the local major normal faults in the region. The results also indicate that bedding attitudes and maximum anisotropy directions are almost parallel or perpendicular to each other. Considering the extensional regime in the regions it is safe to assume that the tilting of the bedding is the result of normal faulting and therefore the strikes of the faults, and the beds are almost parallel to each other as well as they are either perpendicular or parallel to the mean AMS lineations.

In order to obtain mean AMS lineation directions for each domain, the results are categorized based on the ages of host lithologies. The results yielded 12 mean AMS directions for 11 domains (Table 1 and Figure 6). These are produced from a grouping of the Oligocene-Middle Miocene and Late Miocene-Pliocene sequences separately. Obtained mean directions are compared with the length weighted rose diagrams of the normal faults in each domain (Figure 6). The unit length is taken as 250m. As seen in Figure 6, except for Fethiye and Ören sites, in all other domains, the mean AMS directions are either near parallel or near perpendicular to the normal faults. The perpendicular directions are interesting because they indicate major extension directions during and after the deposition of the host lithologies although, the main basin bounding normal faults are perpendicular to the extension directions. In Figure 8, AMS ellipsoids based on the shape factor (T in Table 1) are given. Pre-Late Miocene rocks in Ören and Elmalı domains show prolate NW-SE directed extension while Tavas and Fethiye show almost oblate deformation pattern with major axes-oriented NW-SE similar to other pre-Late Miocene sites. However, magnitudes of principal AMS axes, in other words, strain axes in almost all Late Miocene-Pliocene sites, are almost the same, although their orientations vary.

Using the general trends of the AMS lineations (k_{max}), smoothed trajectories are constructed manually for the Late Miocene-Pliocene (Figure 7). As seen on the figure, the mean AMS lineations, hence maximum extension directions in the Didim, Tavas, Burdur, and Fethiye, are parallel to the smoothed trajectories while Ulubey is perpendicular, and the Acıpayam and Çameli domains are oblique. The obliquity of the Çameli and Acıpayam domains is possibly due to dextral shear associated with the Acıpayam Transfer Zone (Kaymakcı et al., 2018).

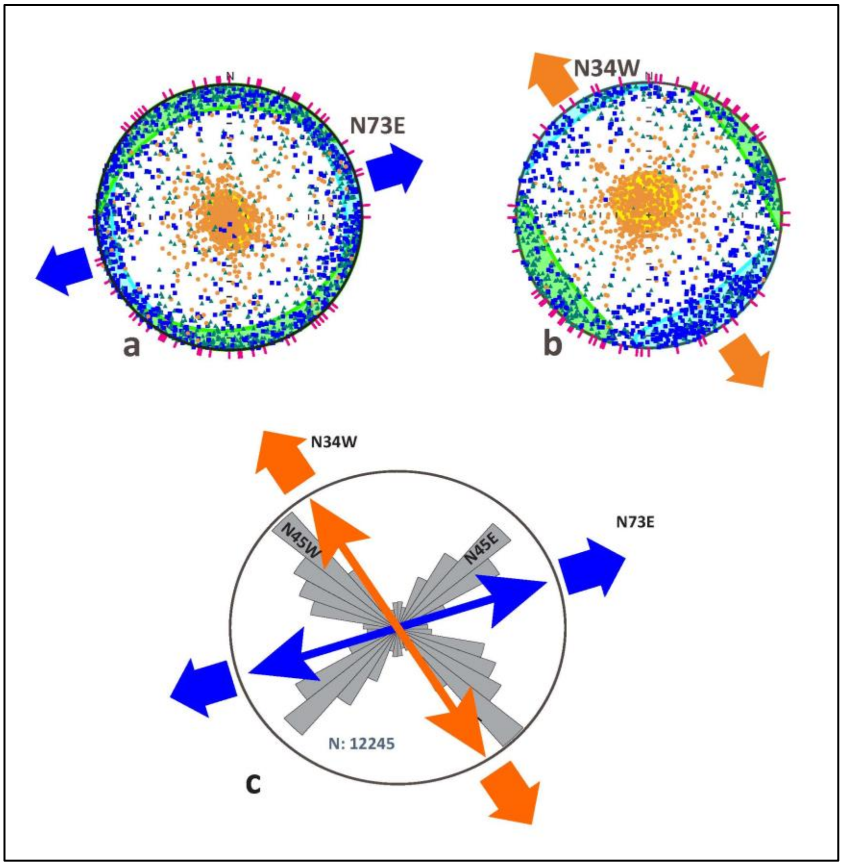

Figure 8. Lower hemisphere equal area plots of axes of the anisotropy of the magnetic susceptibility for Oligocene-Middle Miocene and Late Miocene-Pliocene sites combined.

4.2. Regional implications

The analysis of the results indicates two spatiotemporally distinct directions. The Oligocene-Middle Miocene domains indicate approximately NW-SE directed extension, while Late Miocene-Pliocene domains indicate NE-SW directed extension (Figure 8), which are almost perpendicular to each other. This relationship implies that dominant extension direction has changed in the region from NW-SE to NE-SW by the end of Middle Miocene, however recent field data (Kaymakcı, 2006), moment tensor solutions (Tan et al., 2008; Shah, 2015) and GPS vectors (Elitez et al., 2016) indicate that the region is under the influence of multidirectional extension. However, NE-SW and NW-SE directed extension directions dominate over others.

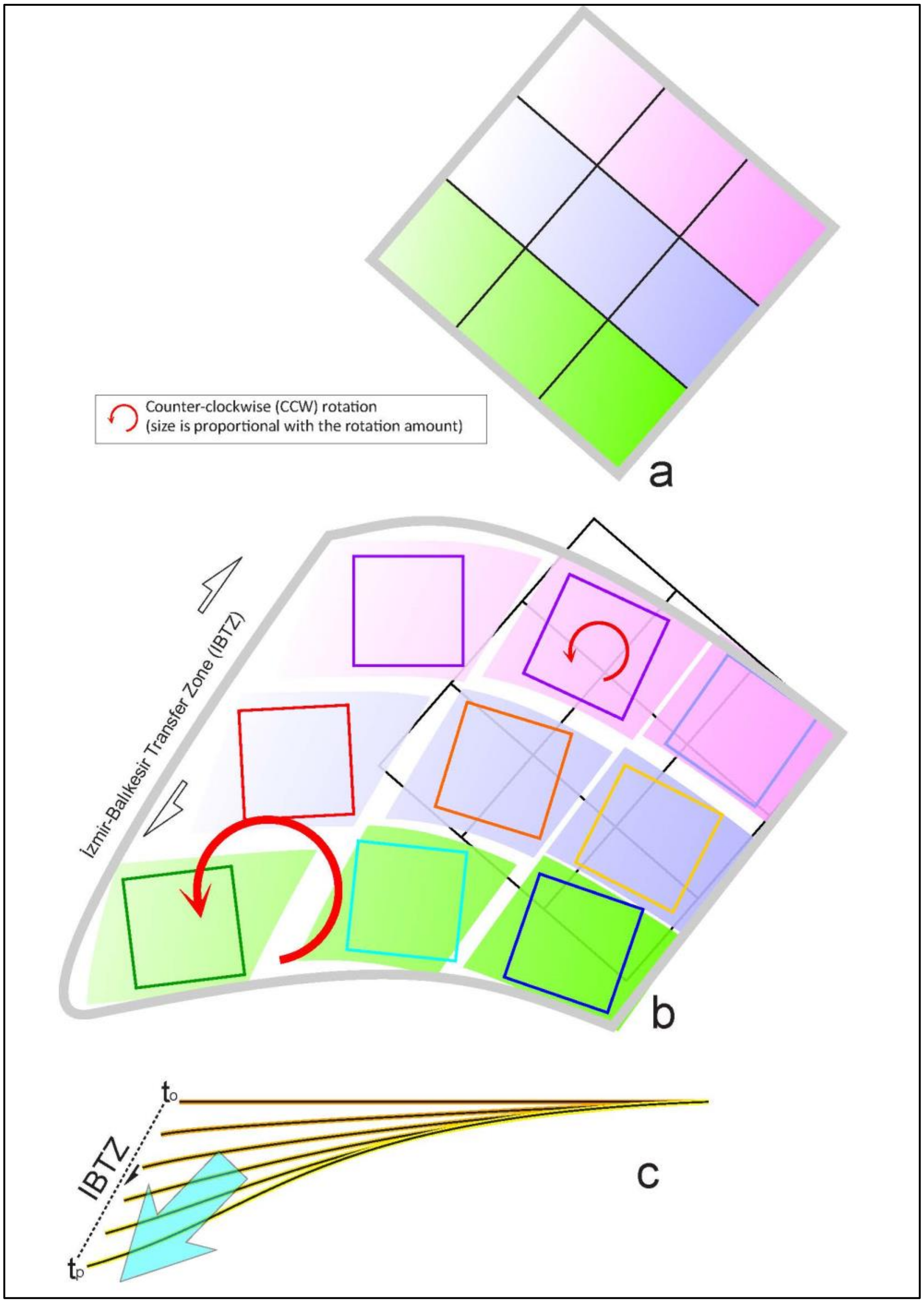

Figure 9. SW Stretching rubber sheet deformation model and counterclockwise rotation amount proposed for SW Anatolia. a) original geometry, b) deformed geometry, c) position of an E-W imagery line during the Oligocene (t_o), and the present (t_p). The arrow shows the main stretching direction. NE corner of the model approximately corresponds to the Burdur domain. Note the change in the shapes of originally square blocks. Rotation senses and amounts, and the rubber sheet model is adopted from Kaymakcı et al. (2018).

The Miocene exhumation of metamorphic core complexes in the region is associated with the extensional deformation resulted from southwards retreat of the northwards subducted African slab below the western Anatolian and the Aegean region (Gessner et al., 2013; Uzel et al., 2015; Kaymakcı et al., 2018). Its exhumation in associated with the exhumation of the Cycladic Complex in the south. The extensional strain between these complexes is coupled with the development of a crustal-scale İzmir-Balıkesir Transfer Zone (İBTZ), dominated by transtensional deformation (Uzel et al., 2013, 2015; Westerweel et al., 2020). On the eastern side of the Menderes Core Complex, a similar transtensional shear zone, namely Fethiye-Burdur Shear Zone (Hall et al., 2014) have also been proposed. However, some authors criticized the presence and proposed sinistral nature of this zone (e.g., Alçiçek, 2015; Kaymakcı et al., 2018; Özkaptan et al., 2018) and argued that such a shear zone would produce strike-slip kinematic indicators, although documented features are mainly related with normal faulting along the proposed zone (Özkaptan et al., 2018), unlikely the İBTZ (e.g., Uzel et al., 2013; 2015; Westerweel, 2020). Besides, a very prominent differential rotation within and outside of such a shear zone would have been developed (Kaymakcı et al., 2018).

However, the AMS results, presented here, indicate smooth transitions of the principal strain axes in the region, which does not corroborate the presence of a strike-slip shear zone in the region.

Paleomagnetic studies carried out in same Neogene sequences in the region (Alçiçek et al., 2016; Gürsoy et al., 2003; Kaymakcı et al., 2018; Kissel & Laj, 1988; Koç et al., 2016; Özkaptan et al., 2014; Tatar et al., 2002; Uzel et al., 2015) as well as, a few magnetostratigraphic studies (Özkaptan et al., 2018; Şen & Seyitoğlu, 2009) and the studies based on fault kinematics, seismotectonic and GNSS based active deformation studies in the region indicate multi-directional extension (Aktuğ et al., 2009; Alçiçek, 2007; Alçiçek et al., 2005, 2006, 2012, 2013, 2018; Barka & Reilinger, 1997; Kaymakcı et al., 2018; Price & Scott, 1994; Taymaz & Price, 1992; ten Veen et al., 2009).

There is a major change in the orientation of the AMS lineations to the north and the south of major domain boundary that is defined approximately by Büyük Menderes-Denizli-Baklan grabens in the west, and Dinar-Aksu faults (Kaymakcı et al. 2018) in the east (Figure 7). This boundary also marks the boundary between clockwise and counterclockwise rotating regions in western Anatolia (Kaymakcı et al. 2018). To this end, we propose that differential extension and rotation deformation in the region gave way to the development of small checkerboard-like faults blocks, south of this line, rotating and translation of which has been produced complex deformation and even locally contrasting deformation styles in the region. Rotation and non-rigid deformation resulted in both inhomogeneous strain and development of discrete shear (transfer) zones between these blocks that have been shaping deformation style and tectonic pattern in the region.

In conclusion, the tectonic style and amount of crustal deformation in SW-Anatolia is revealed by rigorous AMS results obtained from the region. It is found that the variations in the deformation axes are gradually changing between the domains, while the strain shape factor is almost the same all over the Late Miocene-Pliocene sequences. Based on these results and the literature (e.g., Kaymakcı et al., 2018, and references therein), we conclude that the SW Anatolia is under the control of multi-directional extension associated with counterclockwise rotation exerted by the southwards retreat of Eastern Mediterranean subduction system. This resulted in stretching of the SW Anatolia, the over-riding plate, to accommodate the retreat of the trench by a non-rigid stretched rubber-sheet like deformation style (Figure 9), which seems to be pulled from a single point towards SW direction (Kaymakcı et al., 2018). The Büyük Menderes-Denizli-Baklan grabens and Dinar-Aksu faults mark the northern boundary of this peculiar deformation zone.

Conclusions

The tectono-sedimentary magnetic fabrics in the Oligocene - Pliocene basins in SW Anatolia suggest that the original sedimentary (purely compactional) fabrics of these sediments have been overprinted by increasing strain effects closely linked to the Cenozoic tectonic activity.

- The distinct AMS pattern is the result of tectonic deformation; hence they are parallel to the principal strain axes in the region, such that k_{max} corresponds to major extension direction, k_{int} corresponds to intermediate extension direction, and $k_{min,}$ which is almost normal to the bedding, correspond to the compaction.
- Anisotropy of magnetic susceptibility (AMS) results from weakly deformed Oligocene to Pliocene sedimentary rocks from 83 sites dispersed over entire SW Anatolia reveal two dominant extension directions. These are, Oligocene-Middle Miocene NW-SE directed extension and Late Miocene-Pliocene NE-SW directed extension.
- The major extension directions both on-site basis and combined analysis of the sites into deformation domains are generally parallel or perpendicular to the major faults in each domain and bedding strikes.
- Deformation in SW Anatolia is characterized by multi-directional extension with the dominance of NE-SW and NW-SE directions. It is associated with the southwards retreat of the trench related to the eastern Mediterranean subduction system, which resulted in the SW stretched rubber sheet-like deformation of SW Anatolia.
- The obtained results do not endorse the presence of a major sinistral shear zone within the region.

Acknowledgments

This study is supported by the Scientific and Technical Research Council of Turkey (TÜBİTAK) Grant Number ÇAYDAG-111Y239. We would like to thank Pınar Ertepınar, Ayten Koç, and Côme Lefebvre for their support during sample collection in the field. All the data presented here is completely new, and we have not used any AMS data from the literature nor any repositories.

References

Aktuğ, B., Nocquet, J. M., Cingöz, A., Parsons, B., Erkan, Y., England, P., et al. (2009). Deformation of western Turkey from a combination of permanent and campaign GPS data: Limits to block-like behavior. *Journal of Geophysical Research: Solid Earth*, 114(B10). https://doi.org/10.1029/2008JB006000

Alçiçek, M. C. (2007). Tectonic development of an orogen-top rift recorded by its terrestrial sedimentation pattern: The Neogene Eşen Basin of southwestern Anatolia, Turkey. *Sedimentary Geology*, 200(1–2), 117–140. https://doi.org/10.1016/j.sedgeo.2007.04.003

Alçiçek, M. C. (2015). Comment on ‘The Fethiye-Burdur Fault Zone: A component of upper plate extension of the Subduction Transform Edge Propagator fault linking Hellenic and Cyprus Arcs, Eastern Mediterranean. Tectonophysics 635, 80-99’ by J. Hall, A.E. Aksu, I. Elitez, C. Yaltırak. *Tectonophysics*, 664, 1–4. https://doi.org/10.1016/j.tecto.2015.01.025

Alçiçek, M. C., Brogi, A., Capezzuoli, E., Liotta, D., & Meccheri, M. (2013). Superimposed basin formation during Neogene-Quaternary extensional tectonics in SW-Anatolia (Turkey): Insights from the kinematics of the Dinar Fault Zone. *Tectonophysics*, 608(November 2013), 713–727. https://doi.org/10.1016/j.tecto.2013.08.008

Alçiçek, M. C., Kazanci, N., & Özkul, M. (2005). Multiple rifting pulses and sedimentation patterns in the Çameli Basin, southwestern Anatolia, Turkey. *Sedimentary Geology*, 173, 409–431.

Alçiçek, M. C., Mayda, S., & Alçiçek, H. (2012). Faunal and palaeoenvironmental changes in the çal Basin, SW Anatolia: Implications for regional stratigraphic correlation of late Cenozoic basins. *Comptes Rendus - Geoscience*, 344(2), 89–98. https://doi.org/10.1016/j.crte.2012.01.003

Alçiçek, M. C., Mayda, S., & Arzu Demirel, F. (2016). Discussion on ``Neogene-Quaternary evolution of the Tefenni basin on the Fethiye-Burdur fault zone, SW Anatolia-Turkey. Journal of African Earth Science 118, 137-148’’ by R. Aksoy, S. Aksarı; *Journal of African Earth Sciences*. https://doi.org/10.1016/j.jafrearsci.2016.07.024

Alçiçek, M. C., Mayda, S., ten Veen, J. H., Boulton, S. J., Neubauer, T. A., Alçiçek, H., et al. (2019). Reconciling the stratigraphy and depositional history of the Lycian orogen-top basins, SW Anatolia. *Palaeobiodiversity and Palaeoenvironments*, 99(4). https://doi.org/10.1007/s12549-019-00394-3

Alçiçek, M. C., ten Veen, J. H., & Özkul, M. (2006). Neotectonic development of the Çameli Basin, southwestern Anatolia, Turkey. In A. H. F. Robertson & D. Mountrakis (Eds.), *Tectonic Development of the Eastern Mediterranean Region*. Geological Society, London, Special Publications (Vol. 260, pp. 591–611).

Alçiçek, M. C., van den Hoek Ostende, L. W., Saraç, G., Tesakov, A. S., Murray, A. M., Hakyemez, H. Y., et al. (2018). Comment on “Miocene to Quaternary tectonostratigraphic evolution of the middle section of the Burdur-Fethiye Shear Zone, south-western Turkey: Implications for the wide inter-plate shear zones. *Tectonophysics* 690, 336–354”. Tectonophysics, 722, 595–600. https://doi.org/10.1016/J.TECTO.2017.05.027

Barka, A. A., & Reilinger, R. (1997). Active tectonics of the Eastern Mediterranean Region: deduced from GPS, neotectonic and seismic data. *Annali Di Geofisica*, XL(June), 587–6190. https://doi.org/10.1111/j.1365-2486.2011.02460.x

Biryol, C., Beck, S. L., Zandt, G., & Özacar, A. A. (2011). Segmented African lithosphere beneath the Anatolian region inferred from teleseismic P-wave tomography. *Geophysical Journal International*, 184(3), 1037–1057. https://doi.org/10.1111/j.1365-246X.2010.04910.x

Borradaile, G. J. (1988). Magnetic susceptibility, petrofabrics, and strain. *Tectonophysics*. https://doi.org/10.1016/0040-1951(88)90279-X

Borradaile, G. J. (1991). Correlation of strain with anisotropy of magnetic susceptibility (AMS). *Pure and Applied Geophysics*, 135(1), 15–29. https://doi.org/10.1007/BF00877006

Borradaile, G. J., & Henry, B. (1997). Tectonic applications of magnetic susceptibility and its anisotropy. *Earth-Science Reviews*, 42(1–2), 49–93. https://doi.org/10.1016/S0012-8252(96)00044-X

Borradaile, G. J., & Jackson, M. (2010). Structural geology, petrofabrics, and magnetic fabrics (AMS, AARM, AIRM). *Journal of Structural Geology*. https://doi.org/10.1016/j.jsg.2009.09.006

Chadima, M., & Jelinek, V. (2009). *Anisoft 4.2: anisotropy data browser for windows*. Agico. Inc, Brno.

Cifelli, F., Mattei, M., Chadima, M., Hirt, A. M., & Hansen, A. (2005). The origin of tectonic lineation in extensional basins: Combined neutron texture and magnetic analyses on 'undeformed' clays. *Earth and Planetary Science Letters*, 235, 62–78.

Cifelli, F., Mattei, M., Hirt, A. M., & Günther, A. (2004). The origin of tectonic fabrics in 'undeformed' clays: The early stages of deformation in extensional sedimentary basins. *Geophysical Research Letters*, 31(9), 2–5. https://doi.org/10.1029/2004GL019609

Collinson, D. W. (1983). *Methods in Rock Magnetism and Palaeomagnetism. Paleomagnetism-techniques and instrumentation*. London: Chapman & Hall.

Dankers, P. H. M., *Magnetic properties of dispersed natural iron-oxides of known grain-size*, PhD thesis, pp. 143, Rijksuniversiteit te Utrecht, Utrecht, the Netherlands, 1978.

Duermeijer, C. E. E., van Vugt, N., Langereis, C. G. G., Meulenkamp, J. E. E., & Zachariasse, W. J. J. (1998). A major late Tortonian rotation phase in the Crotone basin using AMS as tectonic tilt correction and timing of the opening of the Tyrrhenian basin. *Tectonophysics*, 287(1–4), 233–249. https://doi.org/10.1016/S0040-1951(98)80071-1

Elitez, İ., Yaltırak, C., & Aktuğ, B. (2016). Extensional and compressional regime driven left-lateral shear in southwestern Anatolia (eastern Mediterranean): The Burdur-Fethiye Shear Zone. *Tectonophysics*, 688, 26–35. https://doi.org/10.1016/j.tecto.2016.09.024

Fabian, K., Shcherbakov, V. P., & McEnroe, S. A. (2013). Measuring the Curie temperature. *Geochemistry, Geophysics, Geosystems*, 14(4), 947–961. https://doi.org/10.1029/2012GC004440

Faccenna, C., Bellier, O., Martinod, J., Piromallo, C., & Regard, V. (2006). Slab detachment beneath eastern Anatolia: A possible cause for the formation of the North Anatolian Fault. *Earth and Planetary Science Letters*, 242, 85–97. https://doi.org/10.1016/j.epsl.2005.11.046

Gong, Z., van Hinsbergen, D. J. J., Vissers, R. L. M., & Dekkers, M. J. (2009). Early Cretaceous syn-rotational extension in the Organya basin-New constraints on the palinspastic position of Iberia during its rotation. *Tectonophysics*, 473(3–4), 312–323. https://doi.org/10.1016/j.tecto.2009.03.003

Govers, R., & Wortel, M. J. R. (2005). Lithosphere tearing at STEP faults: Response to edges of subduction zones. *Earth and Planetary Science Letters*, 236, 505–523.

Graham, J. (1966). Significance of magnetic anisotropy in Appalachian sedimentary rocks. American Geophysical Union, *Geophysical Monograph Series*, 627–648.

Gürsoy, H., Piper, J. D. A., & Tatar, O. (2003). Neotectonic deformation in the western sector of tectonic escape in Anatolia: palaeomagnetic study of the Afyon region, central Turkey. *Tectonophysics*, 374(1–2), 57–79. https://doi.org/10.1016/S0040-1951(03)00346-9

Hall, J., Aksu, A. E., Elitez, I., Yaltirak, C., Çifçi, G., & Yaltırak, C. (2014). The Fethiye–Burdur Fault Zone: A component of upper plate extension of the subduction transform edge propagator fault linking Hellenic and Cyprus Arcs, Eastern Mediterranean. *Tectonophysics*, 635, 80–99. https://doi.org/10.1016/j.tecto.2014.05.00

Hayward, A. B. (1984). Sedimentation and basin formation related to ophiolite nappe emplacement, Miocene, SW Turkey. *Sedimentary Geology*, 71, 105–129.

Hirt, A. M., Evans, K. F., & Engelder, T. (1995). Correlation between magnetic anisotropy and fabric for Devonian shales on the Appalachian Plateau. *Tectonophysics*, 247(1–4), 121–132. https://doi.org/10.1016/0040-1951(94)00176-A

Hirt, A. M., Lowrie, W., Clendenen, W. S., & Kligfield, R. (1993). Correlation of strain and the anisotropy of magnetic susceptibility in the Onaping Formation: evidence for a near-circular origin of the Sudbury Basin. *Tectonophysics*, 225(4), 231–254. https://doi.org/10.1016/0040-1951(93)90300-9

Hrouda, F. (1991). Models of magnetic anisotropy variations in sedimentary thrust sheets. *Tectonophysics*, 185(3–4), 203–210. https://doi.org/10.1016/0040-1951(91)90444-W

Hrouda, F. (1993). Theoretical models of magnetic anisotropy to strain relationship revisited. *Physics of the Earth and Planetary Interiors*, 77(3–4), 237–249. https://doi.org/10.1016/0031-9201(93)90101-E

Jelínek, V. (1977). The Statistical Theory of Measuring Anisotropy of Magnetic Susceptibility of Rocks and Its Application. *Geofyzika*.

Jelínek, V. (1978). Statistical processing of magnetic susceptibility measured on groups of specimens. Stud. *Geophys. Geod*, 22, 50–62.

Jelinek, V. (1981). Characterization of the magnetic fabric of rocks. *Tectonophysics*, 79(3–4), T63–T67.

Kaymakcı, N. (2006). Kinematic development and paleostress analysis of the Denizli Basin (Western Turkey): implications of spatial variation of relative paleostress magnitudes and orientations. *Journal of Asian Earth Sciences*, 27(2), 207–222.

Kaymakcı, N., Langereis, C., Özkaptan, M., Özacar, A. A., Gülyüz, E., Uzel, B., & Sözbilir, H. (2018). Paleomagnetic evidence for upper plate response to a STEP fault, SW Anatolia. *Earth and Planetary Science Letters*, 498. https://doi.org/10.1016/j.epsl.2018.06.022

Kissel, C., & Laj, C. (1988). The tertiary geodynamical evolution of the Aegean arc: a paleomagnetic reconstruction. *Tectonophysics*, 146, 183–201.

Kissel, C., Barrier, E., Laj, C., & Lee, T. Q. (1986). Magnetic fabric in “undeformed” marine clays from compressional zones. *Tectonics*, 5(5), 769–781. https://doi.org/10.1029/TC005i005p00769

Koç, A., van Hinsbergen, D. J. J., Kaymakci, N., & Langereis, C. G. (2016). Late Neogene oroclinal bending in the central Taurides: A record of terminal eastward subduction in southern Turkey. *Earth and Planetary Science Letters*, 434, 75–90. https://doi.org/10.1016/J.EPSL.2015.11.020

Kodama, K. P. (1995). Remanence anisotropy as a correction for inclination shallowing: a case study of the Nacimiento Formation. *Eos, Transactions of the American Geophysical Union*, 76, 160–161.

Konak, N., & Şenel, M. (2002). *1/500.000 Scale Geological Map of Turkey, İzmir Sheet.* General Directorate of Mineral Research and Exploration (MTA) Ankara, Turkey.

Le Pichon, X., & Angelier, J. (1979). The Hellenic arc and trench system: a key to the neotectonic evolution of the Eastern Mediterranean area. *Tectonophysics*, 60, 1–42.

Maffione, M., Hernandez-Moreno, C., Ghiglione, M. C., Speranza, F., van Hinsbergen, D. J. J. J., & Lodolo, E. (2015). Constraints on deformation of the Southern Andes since the Cretaceous from anisotropy of magnetic susceptibility. *Tectonophysics*, 665, 236–250. https://doi.org/10.1016/j.tecto.2015.10.008

Maffione, M., Pucci, S., Sagnotti, L., & Speranza, F. (2012). Magnetic fabric of Pleistocene continental clays from the hanging-wall of an active low-angle normal fault (Altotiberina Fault, Italy). *International Journal of Earth Sciences*, 101(3), 849–861. https://doi.org/10.1007/s00531-011-0704-9

Mattei, M., Sagnotti, L., Faccenna, C., & Funiciello, R. (1997). Magnetic fabric of weakly deformed clay-rich sediments in the Italian peninsula: Relationship with compressional and extensional tectonics. *Tectonophysics*, 271(1–2), 107–122. https://doi.org/10.1016/S0040-1951(96)00244-2

Mullender, T. A. T., Frederichs, T., Hilgenfeldt, C., Groot, L. V. de, Fabian, K., & Dekkers, M. J. (2016). Automated paleomagnetic and rock magnetic data acquisition with an in-line horizontal '"2G"' system. *Geochemistry Geophysics Geosystems*, 17, 2825–2834. https://doi.org/10.1002/2016GC006406

Mullender, T. A. T., Van Velzen, A. J., & Dekkers, M. J. (1993). Continuous drift correction and separate identification of ferrimagnetic and paramagnetic contribution in thermamagnetic runs. *Geophysical Journal International*, 114, 663–672.

Noltimier, H. C. (1971). Magnetic rock cylinders with negligible shape anisotropy. *Journal of Geophysical Research*, 76(17), 4035–4037.

Özkaptan, M., & Gülyüz, E. (2019). Relationship between the anisotropy of magnetic susceptibility and development of the Haymana Anticline, Central Anatolia (Turkey). *Turkish Journal of Earth Sciences*, 28(1), 103–121.

Özkaptan, M., Kaymakci, N., Langereis, C. G., Gülyüz, E., Arda Özacar, A., Uzel, B., & Sözbilir, H. (2018). Age and kinematics of the Burdur Basin: Inferences for the existence of the Fethiye Burdur Fault Zone in SW Anatolia (Turkey). *Tectonophysics*, 744. https://doi.org/10.1016/j.tecto.2018.07.009

Özkaptan, M., Koç, A., Lefebvre, C., Gülyüz, E., Uzel, B., Kaymakcı, N., et al. (2014). Kinematics of SW Anatolia implications on crustal deformation above slab tear. In *EGU General Assembly Conference* Abstracts (Vol. 16, p. 6061).

Parés, J. M., & van der Pluijm, B. A. (2002). Phyllosilicate fabric characterization by Low-Temperature Anisotropy of Magnetic Susceptibility (LT-AMS). *Geophysical Research Letters*, 29(24), 68-1-68–4. https://doi.org/10.1029/2002GL015459

Parés, J. M., Van der Pluijm, B. A., & Dinarès-Turell, J. (1999). Evolution of magnetic fabrics during incipient deformation of mudrocks (Pyrenees, northern Spain). *Tectonophysics*, 307(1–2), 1–14. https://doi.org/10.1016/S0040-1951(99)00115-8

Passier, H. F., De Lange, G. J., & Dekkers, M. J. (2001). Magnetic properties and geochemistry of the active oxidation front and the youngest sapropel in the eastern Mediterranean sea. *Geophysical Journal International*, 145(3), 604–614. https://doi.org/10.1046/j.0956-540X.2001.01394.x

Price, S. P., & Scott, B. C. (1994). Fault-block rotations at the edge of a zone of continental extension, southwest Turkey. *Journal of Structural Geology*, 16, 381–392.

Ramsey, J. G., & Huber, M. I. (1983). *Instructor's Manual to Accompany the Techniques of Modern Structural Geology*, Volume 1, Strain Analysis. Acad. Press.

Rochette, P. (1987). Magnetic susceptibility of the rock matrix related to magnetic fabric studies. *Journal of Structural Geology*, 9(8), 1015–1020. https://doi.org/10.1016/0191-8141(87)90009-5

Rochette, P., Jackson, M., & Aubourg, C. (1992). Rock magnetism and the interpretation of anisotropy of magnetic susceptibility. *Reviews of Geophysics*, 30(3), 209–226.

Sagnotti, L., & Speranza, F. (1993). Magnetic fabric analysis of the Plio-Pleistocene clayey units of the Sant'Arcangelo basin, southern Italy. *Physics of the Earth and Planetary Interiors*, 77(3–4), 165–176. https://doi.org/10.1016/0031-9201(93)90096-R

Sagnotti, L., Faccenna, C., Funiciello, R., & Mattei, M. (1994). Magnetic fabric and structural setting of Plio–Pleistocene clayey units in an extensional regime: the Tyrrhenian margin of central Italy. *Journal of Structural Geology*, 16, 1243–1257.

Scheepers, P. J. J., & Langereis, C. G. (1994). Magnetic fabric of Pleistocene clays from the Tyrrhenian Arc; a magnetic lineation induced in the final stage of the middle Pleistocene compressive event. *Tectonics*, 13(5), 1190–1200.

Scriba, H., & Heller, F. (1978). Measurements of anisotropy of magnetic susceptibility using inductive magnetometers. *J. Geophys*, 44, 341–352.

Şen, Ş., & Seyitoğlu, G. (2009). Magnetostratigraphy of early-middle Miocene deposits from E-W trending Alasehir and Büyük Menderes grabens in western Turkey, and its tectonic implications. In D. J. J. van Hinsbergen, M. A. Edwards, & R. Govers (Eds.), *Collision and collapse at the Africa-Arabia-Eurasia subduction zone*: Geological Society of London Special Publication (Vol. 311, pp. 321–342).

Şenel, M. (2002). *1/500.000 Scale Geological Map of Turkey, İzmir, Ankara, Denizli and Konya Sheets*. General Directorate of Mineral Research and Exploration (MTA) Ankara, Turkey.

Şengör, A. M. ., Tüysüz, O., İmren, C., Sakınç, M., Eyidoğan, H., Görür, N., et al. (2005). the North Anatolian Fault: a New Look. *Annual Review of Earth and Planetary Sciences*, 33(1), 37–112. https://doi.org/10.1146/annurev.earth.32.101802.120415

Shah, S. T. (2015). Stress tensor inversion from focal mechanism solutions and earthquake probability analysis of Western Anatolia, Turkey, METU MSc Thesis. http://etd.lib.metu.edu.tr/upload/12618444/index.pdf.

Shah, S.T., Özacar, A.A. (2018). Spatial Variations of Active Stress Patterns and Frequency-Magnitude Distribution of Earthquakes in Western Anatolia, Turkey. *Proceedings of 71st Geological Congress of Turkey*, 23-27 April 2018, METU, Ankara, Turkey

Soto, R., Larrasoaña, J. C., Arlegui, L. E., Beamud, E., Oliva-Urcia, B., & Simón, J. L. (2009). Reliability of magnetic fabric of weakly deformed mudrocks as a palaeostress indicator in compressive settings. *Journal of Structural Geology*, 31(5), 512–522. https://doi.org/10.1016/j.jsg.2009.03.006

Tan, O., Tapirdamaz, M. C., & Yörük, A. (2008). The earthquake catalogues for Turkey. *Turkish Journal of Earth Sciences*. *17*(2), 405-418.

Tarling, D., & Hrouda, F. (1993). *Magnetic Anisotropy of Rocks*. (D. Tarling & F. Hrouda, Eds.) (1st ed.). Springer Netherlands.

Tatar, O., Gürsoy, H., & Piper, J. D. A. (2002). Differential neotectonic rotations in Anatolia and the Tauride Arc: p[alaeomagnetic investigation of the Erenlerdag Volcanic Omplex and Isparta volcanic district, south-central Turkey. *Journal of the Geological Society of London*, 159, 281–294.

Taymaz, T., & Price, S. (1992). May 12 Burdur earthquake sequence, SW Turkey: a synthesis of seismological and geological observations. *Geophysical Journal International*, 108, 589–603.

ten Veen, J., H. (2004). Extension of Hellenic forearc shear zones in SW Turkey: the Pliocene–Quaternary deformation of the Eşen Çay Basin. Journal of Geodynamics, 37(2), 181-204.

ten Veen, J. H., Boulton, S. J., & Alçiçek, M. C. (2009). From palaeotectonics to neotectonics in the Neotethys realm: The importance of kinematic decoupling and inherited structural grain in SW Anatolia (Turkey). *Tectonophysics*, 473(1–2), 261–281. https://doi.org/10.1016/j.tecto.2008.09.030

Uzel, B., Langereis, C. G., Kaymakci, N., Sözbilir, H., Özkaymak, Ç., & Özkaptan, M. (2015). Paleomagnetic evidence for an inverse rotation history of Western Anatolia during the exhumation of Menderes core complex. *Earth and Planetary Science Letters*, 414, 108–125.

Uzel, B., Sözbilir, H., Özkaymak, Ç., Kaymakcı, N., & Langereis, C. G. (2013). Structural evidence for strike-slip deformation in the Izmir–Balıkesir transfer zone and consequences for late Cenozoic evolution of western Anatolia (Turkey). *Journal of Geodynamics*, 65, 94–116.

van Hinsbergen, D. J. J., Dekkers, M. J., Bozkurt, E., & Koopman, M. (2010). Exhumation with a twist: Paleomagnetic constraints on the evolution of the Menderes metamorphic core complex, western Turkey. *Tectonics*, 29(3), 1–33. https://doi.org/10.1029/2009TC002596

van Hinsbergen, D. J. J., Kaymakcı, N., Spakman, W., & Torsvik, T. H. (2010). Reconciling the geological history of western Turkey with plate circuits and mantle tomography. *Earth and Planetary Science Letters*, 297(3), 674–686.

Westerweel, J., Uzel, B., Langereis, C. G., Kaymakci, N., & Sözbilir, H. (2020). Paleomagnetism of the Miocene Soma basin and its structural implications on the central sector of a crustal-scale transfer zone in western Anatolia (Turkey). Journal of Asian Earth Sciences, 193. https://doi.org/10.1016/j.jseaes.2020.104305

Wortel, M. J. R., & Spakman, W. (2000). Subduction and slab detachment in the Mediterranean-Carpathian region. *Science*, 290, 1910–1917.

Table Caption

Table 1. Early Miocene to Pliocene anisotropy of magnetic susceptibility results from the SW Anatolia locations.

Figure captions

Figure 1. a) Simplified tectonic scheme of the eastern Mediterranean region. b) simplified geological map of SW Anatolia showing AMS sample locations and major faults (MTA, 2002 and Kaymakcı et al., 2018).

Figure 2. Representative thermomagnetic curves for each site, consisting of several heating-cooling cycles to asses changes (alterations) in the magnetic properties (Mullender et al., 1993). The final cooling curve is indicated with the blue line. See the text for an explanation of the thermomagnetic behavior.

Figure 3. a) Frequency distribution of the magnetic susceptibility (km) from all measured specimens. b) Anisotropy plots of magnetic foliation (F) versus magnetic lineation (L). c) Shape factor (T) versus corrected anisotropy degree (Pj) diagram compared to the typical trend expected from an increasing degree of deformation, from an oblate sedimentary magnetic fabric (I) to a prolate tectonic-sedimentary fabric (II) and finally to an oblate purely tectonic fabric.

Figure 4. The orientations of site mean magnetic lineations (kmax) after bedding plane correction per site.

Figure 5. Lower hemisphere equal area plots of the three axes of the anisotropy of the magnetic susceptibility ellipsoids from the 11 domains after bedding plane correction. The site-based AMS results are given in Table 1.

Figure 6. The orientation of the mean magnetic lineation (k_{max}) of each 11 domains after tectonic correction overlaid on length weighted rose diagrams prepared from normal faults for each domain.

Figure 7. Strain ellipses based on directions and relative magnitudes of K_{max} and K_{int} for each domain. Dashed lines are manually constructed smoothed strain trajectories. Note near-identical geometries of Late Miocene-Pliocene strain ellipses and their variations in the Early-Middle Miocene rocks.

Figure 8. Lower hemisphere equal area plots of axes of the anisotropy of the magnetic susceptibility for Oligocene-Middle Miocene and Late Miocene-Pliocene sites combined.

Figure 9. SW Stretching rubber sheet deformation model and counterclockwise rotation amount proposed for SW Anatolia. a) original geometry, b) deformed geometry, c) position of an E-W imagery line during the Oligocene (to), and the present (tp). The arrow shows the main stretching direction. NE corner of the model approximately corresponds to the Burdur domain. Note the change in the shapes of originally square blocks. Rotation senses and amounts, and the rubber sheet model is adopted from Kaymakcı et al. (2018).

Locality	Site	Geog. Coord. (deg) Lat. (N)	Long. (E)	N_{AMS}	Age	Rock	Bedding Strike/dip	$k_{m}*10^{6}$ (SI)	L	F	Pj	T	NTC D/I (k_{max})	D/I (k_{int})	D/I (kMio.n	TC D/I (k_{max})	D/I (k_{int})	D/I (kMio.i	e_1	e_2	e_3
Acıpayam	~~PK2~~	~~37.5845~~	~~29.3505~~	~~16~~	~~Plio.~~	~~limestone~~	~~193/18~~	~~-0005.7~~	~~1.086~~	~~1.079~~	~~1.181~~	~~0.045~~	~~058.9/42.3~~	~~299.1/28.6~~	~~187.3/34.3~~	~~043.0/53.5~~	~~297.4/11.2~~	~~199.7/34.3~~	~~45.2~~	~~54.5~~	~~50.0~~
	PK3	37.4199	29.3424	09	Lt. Mio.	mud-marl	193/18	0082.0	1.005	1.005	1.010	0.030	189.6/05.6	283.9/37.0	092.3/52.4	191.5/06.4	283.7/19.0	083.8/69.8	31.8	29.5	28.2
	PK4	37.3402	29.3659	13	Lt. Mio.	mud-marl	252/10	3240.0	1.007	1.014	1.021	0.250	244.7/04.8	335.0/03.9	103.6/83.8	245.6/06.0	155.0/06.1	020.1/81.4	19.3	35.7	33.1
	EL3	37.2308	29.5361	05	Plio.	mud-marl	138/23	4660.0	1.004	1.011	1.015	0.413	063.3/05.4	154.4/11.7	308.9/77.1	065.2/27.5	157.5/04.5	256.0/62.1	20.5	20.7	06.5
	EL4	37.1866	29.5324	06	Plio.	mud-marl	188/08	5990.0	1.007	1.078	1.095	0.783	275.3/11.8	06.5/05.8	122.1/76.8	275.4/03.8	005.7/05.5	150.7/83.3	47.5	47.5	04.4
Plio.	**mean**			**33**	**Plio.**			**3100.0**	**1.006**	**1.022**	**1.031**	**0.312**	**237.1/05.3**	**327.9/08.8**	**116.31/79.7**	**239.7/0.4**	**329.7/03.5**	**143.8/86.5**	**42.1**	**42.4**	**16.6**
Burdur	BU1	37.6848	30.3129	08	Plio.	mud-marl	090/20	0040.8	1.008	1.009	1.017	0.058	233.5/29.4	141.6/03.4	045.6/60.3	226.9/16.5	320.6/12.2	085.4/69.2	62.1	62.3	31.0
	BU2	37.6218	30.2732	10	Plio.	mud-marl	070/20	0174.0	1.007	1.024	1.033	0.481	245.7/13.2	155.2/02.0	057.0/76.6	241.4/11.0	335.0/18.0	121.5/68.8	18.5	18.8	07.2
	BU3	37.5796	30.1568	06	Plio.	mud-marl	355/19	0076.5	1.003	1.015	1.020	0.663	293.4/11.0	023.9/02.7	127.5/78.6	296.7/27.5	203.3/6.5	101.2/61.6	33.0	32.8	09.1
	RB1	37.7074	30.2925	15	Plio.	mud-sand.	043/11	0012.0	1.019	1.024	1.045	0.167	234.7/11.9	144.5/00.6	051.6/78.1	232.2/13.8	324.7/10.2	089.8/72.7	23.9	23.9	07.5
	RB2	37.7074	30.2925	07	Plio.	mud-sand.	040/16	0031.4	1.008	1.023	1.033	0.439	067.1/02.3	337.0/00.3	239.0/87.7	246.7/05.0	138.3/74.6	138.3/74.6	11.8	13.0	07.5
	SK7	37.4861	30.1595	18	Plio.	mud-marl	036/16	0092.2	1.003	1.020	1.026	0.685	090.0/08.7	180.7/04.4	297.4/80.3	270.4/04.3	000.7/04.9	138.9/83.5	18.2	18.4	07.4
	SK8	37.6389	30.1677	09	Plio.	mud-marl	312/05	0080.8	1.003	1.017	1.021	0.705	131.1/08.9	040.5/04.1	286.2/80.2	130.3/08.8	220.5/00.9	316.5/81.2	65.3	65.3	11.2
	~~SK9~~	~~37.7053~~	~~30.2379~~	~~08~~	~~Plio.~~	~~mud-marl~~	~~035/20~~	~~0006.7~~	~~1.036~~	~~1.027~~	~~1.064~~	~~-0.137~~	~~136.2/12.8~~	~~229.9/15.8~~	~~008.9/69.5~~	~~136.2/12.8~~	~~223.5/19.9~~	~~064.1/68.9~~	~~54.8~~	~~67.3~~	~~67.4~~
	RCM1	37.4689	30.1794	10	Plio.	mud	070/20	0109.0	1.002	1.018	1.022	0.830	100.9/04.9	192.7/20.1	357.9/69.3	280.8/05.5	190.5/03.0	071.8/83.7	23.1	23.2	07.8
	BS	37.7071	30.2926	114	Plio.	mud-marl	070/10	0049.8	1.007	1.019	1.028	0.399	110.9/10.4	201.5/03.2	308.7/79.1	111.6/03.7	021.3/03.7	246.7/84.8	54.5	54.6	15.1
Plio.	**mean**			**197**	**Plio.**		**~048/14**	**0061.3**	**1.007**	**1.019**	**1.028**	**0.446**	**083.5/02.7**	**173.8/07.7**	**334.2/81.8**	**258.6/02.2**	**348.7/02.3**	**124.9/86.8**	**70.3**	**70.3**	**14.4**
Çameli	RMC3	37.0369	29.4547	20	Lt. Mio.-Plio.	clay-sand.	130/10	0010.4	1.043	1.023	1.072	-0.005	098.3/21.7	358.1/24.1	225.4/56.6	102.2/26.7	354.5/31.3	224.3/46.6	47.2	60.0	60.0
	RCM4	37.0236	29.3859	23	Lt. Mio.-Plio.	mud-marl	220/10	0009.1	1.011	1.011	1.023	-0.023	163.4/22.8	256.8/08.1	005.3/65.6	164.7/26.9	257.3/05.1	357.2/62.5	20.6	56.5	56.2
	RCM5	36.9765	29.3600	17	Lt. Mio.-Plio.	mud-marl	220/05	0325.0	1.004	1.008	1.013	0.178	233.7/07.6	324.1/03.2	077.2/81.8	234.4/04.3	144.1/04.1	011.0/84.1	36.7	37.2	20.9
	RCM6	37.0718	29.3126	59	Lt. Mio.-Plio.	clay	210/08	0035.2	1.004	1.015	1.020	0.612	161.9/09.4	068.9/12.9	287.2/74.0	160.9/04.3	070.6/04.4	295.4/83.8	44.5	44.5	07.6
	RCM7	37.0602	29.2394	24	Lt. Mio.-Plio.	clay	012/10	0066.1	1.004	1.018	1.024	0.659	044.4/01.5	314.3/02.4	165.8/87.1	224.4/04.2	314.7/04.2	089.7/84.0	10.5	10.5	05.7
	RCM8	37.0263	29.0185	30	Lt. Mio.-Plio.	clay-sand.	332/06	0061.9	1.002	1.014	1.017	0.703	266.1/17.9	011.0/17.9	156.6/46.0	277.1/13.4	007.5/01.6	104.3/76.5	30.8	31.0	09.1
	RCM9	36.9768	29.2231	35	Lt. Mio.-Plio.	clay	265/38	0016.4	1.012	1.018	1.031	0.218	048.9/48.1	155.0/13.9	256.3/38.5	054.2/09.1	145.9/10.6	284.4/76.0	25.6	25.7	13.8
	RCM10	36.9482	29.1491	43	Lt. Mio.-Plio.	clay	335/40	0067.9	1.007	1.010	1.017	0.193	086.2/19.5	182.3/16.9	310.3/63.7	268.2/0.1	178.2/05.7	359.4/84.2	11.1	11.1	06.1
	PK5	37.2315	29.3070	10	Lt. Mio.-Plio.	mud-marl	350/18	2320.0	1.003	1.014	1.018	0.486	280.5/12.3	011.3/03.3	116.2/77.2	283.1/29.1	191.3/03.2	095.5/60.7	29.7	30.9	20.9
	PK6	37.2099	29.3488	07	Lt. Mio.-Plio.	mud-marl	345/10	0069.3	1.004	1.004	1.008	0.132	107.0/12.9	016.8/01.0	282.5/77.1	106.2/04.3	196.5/04.3	330.9/83.9	49.6	49.4	31.0
	SK5	37.0444	29.5360	17	Lt. Mio.-Plio.	mud-marl	356/29	0146.0	1.005	1.006	1.010	0.093	051.8/14.8	143.8/07.5	259.7/73.3	047.9/01.8	324.0/08.2	094.3/77.5	24.9	30.8	29.6
	SK6	37.1036	29.5265	17	Lt. Mio.-Plio.	mud-marl	320/08	0059.5	1.006	1.009	1.016	0.211	044.7/20.6	312.7/05.4	208.8/68.7	045.0/12.6	313.5/06.3	197.5/75.9	59.6	59.6	14.3
Lt. Mio.-Plio.	**mean**			**295**	**Lt. Mio.-Plio.**		**~320/11**	**0143.0**	**1.006**	**1.012**	**1.019**	**0.347**	**048.2/15.0**	**140.8/09.3**	**261.6/72.2**	**056.0/00.3**	**146.0/02.7**	**319.8/87.3**	**64.4**	**64.4**	**17.5**
Denizli	BD2	37.8168	28.8638	05	Lt. Mio.	marl	028 / 16	0104.0	1.002	1.018	1.022	0.784	126.6/10.3	036.3/01.6	297.3/79.6	306.5/05.5	216.4/00.7	119.4/84.4	19.1	19.1	03.1
	~~BD3~~	~~37.7699~~	~~28.7296~~	~~12~~	~~L.Mio.~~	~~marl~~	~~118 / 22~~	~~0131.0~~	~~1.005~~	~~1.006~~	~~1.012~~	~~-0.029~~	~~213.4/26.3~~	~~119.2/08.4~~	~~013.0/62.2~~	~~212.8/04.3~~	~~122.3/07.3~~	~~333.4/81.5~~	~~52.1~~	~~56.7~~	~~52.2~~
	BD4	37.7329	28.6304	16	Lt. Mio.	marl	+	0023.6	1.010	1.014	1.025	0.183	271.7/06.3	002.3/05.5	132.9/81.6	ii	002.3/05.5	132.9/81.6	54.8	54.5	24.4
	BD5	37.8621	28.6718	10	Lt. Mio.	marl	136 / 24	1330.0	1.018	1.058	1.080	0.536	165.1/01.8	255.6/15.4	068.7/74.5	343.6/09.8	074.6/05.7	194.2/78.7	42.2	42.2	05.2
Lt. Mio.	**mean**			**31**	**Lt. Mio.**		**~136/24**	**0459.0**	**1.011**	**1.029**	**1.042**	**0.394**	**331.2/02.0**	**240.8/10.3**	**331.2/02.0**	**326.1/07.7**	**056.7/04.8**	**178.3/80.9**	**70.1**	**70.1**	**10**
Didim	~~DM1~~	~~37.4776~~	~~27.3436~~	~~25~~	~~Plio.~~	~~lmst~~	~~024/12~~	~~0024.1~~	~~1.104~~	~~1.069~~	~~1.207~~	~~0.055~~	~~147.5/19.9~~	~~258.4/44.6~~	~~040.6/38.7~~	~~145.8/09.8~~	~~249.4/53.9~~	~~049.0/34.4~~	~~29.4~~	~~34.5~~	~~30.1~~
	~~DM2~~	~~37.4127~~	~~27.3755~~	~~27~~	~~Plio.~~	~~lmst~~	~~002/07~~	~~-0006.4~~	~~1.050~~	~~1.033~~	~~1.100~~	~~-0.051~~	~~111.9/03.4~~	~~020.3/26.1~~	~~208.7/63.7~~	~~291.9/03.2~~	~~023.3/23.7~~	~~194.6/66.0~~	~~30.5~~	~~53.1~~	~~52.8~~
	DM3	37.3976	27.2433	21	Plio.	marl	+	1130.0	1.004	1.037	1.045	0.794	117.0/02.3	026.3/04.0	237.4/85.4	117.0/02.3	026.8/04.0	237.4/85.4	41.5	41.5	08.0
	DM4	37.3955	27.3511	27	Plio.	lmst	+	0772.0	1.005	1.007	1.013	0.184	299.2/10.8	209.0/00.9	114.1/79.2	299.2/10.8	209.0/00.9	114.1/79.2	63.1	63.2	37.0
Plio.	**mean**			**48**	**Plio.**		**000/00**	**0927.0**	**1.004**	**1.02**	**1.027**	**0.451**	**120.2/00.2**	**030.2/03.5**	**213.0/86.5**	**120.2/00.2**	**030.2/03.5**	**213.0/86.5**	**59.8**	**59.8**	**11.9**
Dinar	~~BU4~~	~~38.0392~~	~~30.0896~~	~~07~~	~~Plio.~~	~~mud-marl~~	~~080/11~~	~~0050.4~~	~~1.038~~	~~1.358~~	~~1.534~~	~~0.393~~	~~306.2/61.6~~	~~207.1/04.9~~	~~114.5/27.9~~	~~287.1/68.3~~	~~027.0/03.9~~	~~118.5/21.3~~	~~20.5~~	~~20.8~~	~~08.5~~
	~~SK10~~	~~37.9578~~	~~29.8946~~	~~13~~	~~Plio.~~	~~mud-marl~~	~~215/06~~	~~0621.0~~	~~1.008~~	~~1.006~~	~~1.014~~	~~-0.142~~	~~039.0/84.8~~	~~283.9/02.2~~	~~193.8/04.7~~	~~347.6/82.4~~	~~103.9/003.4~~	~~194.3/06.8~~	~~27.8~~	~~33.2~~	~~28.6~~
Plio.	**mean**											**No availble data!**									
Elmalı	ST1	36.4245	29.5558	28	E.-Mid.Mio.	lmst	255/40	1020.0	1.017	1.040	1.060	0.381	296.2/21.8	042.0/34.1	180.0/47.8	120.4/06.2	029.5/08.0	248.0/79.9	31.6	33.7	18.5
	ST2	36.3789	29.5091	33	E.-Mid.Mio.	lmst	231/42	0078.0	1.007	1.018	1.026	0.390	249.6/04.5	344.2/45.4	155.3/44.2	068.0/08.9	337.1/05.6	215.4/79.4	13.1	13.0	07.4
	ST3	36.6075	29.7410	20	E.-Mid.Mio.	lmst	185/45	0305.0	1.011	1.029	1.042	0.430	348.5/16.2	240.3/47.1	091.8/38.4	342.0/00.2	252.0/07.0	073.9/83.0	22.6	22.5	10.7
	ST4	36.3795	29.9363	22	E.-Mid.Mio.	lmst	274/31	0083.7	1.005	1.018	1.025	0.580	300.4/05.0	031.8/15.5	193.1/73.7	119.5/08.8	211.4/12.1	354.2/74.9	15.7	15.7	06.5
	ST5	37.0515	30.1534	20	E.-Mid.Mio.	lmst	220/40	0044.6	1.006	1.020	1.028	0.511	025.1/25.4	284.1/22.0	158.5/55.3	012.5/10.3	105.2/14.5	248.2/72.1	20.4	20.6	12.0
	~~ST6~~	~~37.0387~~	~~30.0888~~	~~09~~	~~E.-Mid.Mio.~~	~~mud-marl~~	~~145/66~~	~~0440.0~~	~~1.029~~	~~1.053~~	~~1.084~~	~~0.292~~	~~181.7/01.8~~	~~272.3/17.1~~	~~085.8/72.8~~	~~343.7/32.2~~	~~100.0/35.1~~	~~223.9/38.3~~	~~03.3~~	~~03.7~~	~~03.7~~
	~~EL1~~	~~36.5159~~	~~29.6760~~	~~08~~	~~E.-Mid.Mio.~~	~~mud-marl~~	~~230/32~~	~~-0004.5~~	~~1.133~~	~~1.113~~	~~1.272~~	~~-0.040~~	~~059.1/05.4~~	~~151.9/27.5~~	~~318.9/61.9~~	~~054.8/09.4~~	~~160.4/58.3~~	~~319.4/29.9~~	~~73.8~~	~~73.8~~	~~58.4~~
	EL2	36.5489	29.6611	05	E.-Mid.Mio.	mud-marl	234/08	0889.0	1.033	1.053	1.089	0.228	006.1/12.1	271.9/19.2	126.4/67.0	005.3/06.1	273.7/14.2	117.8/74.5	03.4	05.2	04.2
	SK3	36.4740	29.6417	05	E.-Mid.Mio.	mud-marl	220/29	0048.0	1.011	1.015	1.027	0.132	323.8/30.6	226.1/12.8	116.2/56.2	321.9/02.3	231.6/08.3	067.4/81.4	13.3	15.2	12.8
	~~SK4~~	~~36.5369~~	~~29.7052~~	~~10~~	~~E.-Mid.Mio.~~	~~mud-marl~~	~~210/21~~	~~0000.2~~	~~1.153~~	~~1.265~~	~~1.496~~	~~-0.092~~	~~331.0/23.9~~	~~066.5/44.1~~	~~222.0/36.4~~	~~328.3/05.6~~	~~068.0/59.8~~	~~235.0/29.6~~	~~82.4~~	~~82.4~~	~~46.7~~
	GM	36.5308	29.6615	316	E.-Mid.Mio.	mud-marl	220/26	0885.0	1.021	1.030	1.053	0.114	320.0/14.2	222.5/27.3	074.5/58.6	142.5/09.5	234.2/10.0	009.8/76.2	30.7	31.2	29.0
E.-Mid. Mio.	**mean**			**33**	**E.-Mid.Mio.**		**~223/29**	**0722.0**	**1.018**	**1.028**	**1.049**	**0.214**	**317.5/18.7**	**221.7/16.7**	**092.8/64.5**	**141.7/07.2**	**232.4/04.9**	**356.1/81.3**	**35.8**	**36.2**	**26.5**
Fethiye	~~FE1~~	~~36.7181~~	~~29.4228~~	~~09~~	~~M.Mio.~~	~~mud-marl~~	~~290/35~~	~~0539.0~~	~~1.023~~	~~1.032~~	~~1.057~~	~~0.136~~	~~015.8/02.8~~	~~284.1/32.2~~	~~110.2/57.7~~	~~195.0/32.1~~	~~305.5/29.1~~	~~067.9/43.9~~	~~25.6~~	~~25.7~~	~~13.7~~
	FE2	36.7098	29.4162	13	M.Mio.	mud-marl	321/20	0127.0	1.008	1.029	1.039	0.580	325.3/14.6	058.6/12.2	186.9/70.8	330.1/12.3	238.5/07.6	117.3/75.5	42.4	42.3	25.2
	FE4	36.4531	29.2902	12	Plio.	mud-marl	045/20	0639.0	1.007	1.012	1.019	0.276	286.1/03.2	016.2/01.0	122.8/86.6	284.0/20.6	018.0/10.4	132.2/66.7	35.8	35.9	22.1
	FE6	36.3603	29.3307	05	Plio.	mud-marl	045/20	0881.0	1.005	1.007	1.013	0.032	130.7/11.0	038.8/09.8	268.1/75.2	310.8/09.0	042.6/11.3	183.1/75.5	71.1	71.2	23.9
	SK1	36.6460	29.3980	09	M.Mio.	mud-marl	215/12	0286.0	1.016	1.042	1.061	0.438	353.9/01.4	263.3/23.5	087.0/66.4	174.3/06.5	266.0/14.4	060.6/74.2	20.8	23.7	13.7
	SK2	36.4622	29.3633	08	Plio.	mud-marl	000/10	3690.0	1.009	1.075	1.093	0.740	029.6/14.9	119.6/00.3	210.9/75.1	031.5/09.8	300.0/08.4	170.2/77.1	32.3	32.3	06.1
Plio.	mean			**25**	**Plio.**		**~030/14**	**1670.0**	**1.007**	**1.031**	**1.042**	**0.376**	**086.5/06.8**	**355.3/10.4**	**209.1/77.5**	**067.3/00.6**	**337.2/14.5**	**159.8/75.5**	**79.1**	**79.1**	**12.9**
M. Mio.				**22**	**M.Mio.**		**~215/12**	**0192.0**	**1.011**	**1.034**	**1.048**	**0.522**	**342.7/10.9**	**251.3/07.2**	**128.6/76.9**	**349.9/01.2**	**259.6/13.5**	**084.7/76.5**	**39.3**	**38.2**	**21.1**
Ören	OR1	37.1673	27.8175	14	E.-Mid. Mio.	mud-marl	089/05	0021.7	1.016	1.015	1.032	-0.082	154.7/07.9	249.8/32.7	052.8/56.1	154.9/03.3	246.9/31.0	059.3/58.8	31.9	56.8	56.8
	~~OR2~~	~~37.1533~~	~~27.8866~~	~~07~~	~~E. Mid. Mio.~~	~~mud-marl~~	~~153/32~~	~~-0005.7~~	~~1.087~~	~~1.079~~	~~1.185~~	~~0.119~~	~~126.7/49.3~~	~~300.67/40.6~~	~~033.2/03.0~~	~~168.0/52.8~~	~~285.9/19.6~~	~~027.9/30.2~~	~~45.6~~	~~45.9~~	~~21.1~~
	~~OR3~~	~~37.0757~~	~~27.9431~~	~~08~~	~~E. Mid. Mio.~~	~~mud-marl~~	~~344/18~~	~~-0008.8~~	~~1.041~~	~~1.075~~	~~1.123~~	~~0.294~~	~~317.2/47.7~~	~~225.6/01.5~~	~~134.3/42.3~~	~~338.3/52.8~~	~~224.2/17.2~~	~~123.1/31.8~~	~~66.7~~	~~65.6~~	~~41.7~~
	~~OR4~~	~~37.0473~~	~~28.0191~~	~~11~~	~~E. Mid. Mio.~~	~~mud-marl~~	~~260/18~~	~~-0002.4~~	~~0.970~~	~~1.008~~	~~1.144~~	~~-0.194~~	~~006.4/20.3~~	~~100.3/17.2~~	~~230.2/62.9~~	~~005.4/03.0~~	~~096.7/23.4~~	~~268.6/66.6~~	~~18.9~~	~~23.8~~	~~25.4~~
	~~OR5~~	~~37.0582~~	~~28.1703~~	~~13~~	~~E. Mid. Mio.~~	~~mud-marl~~	~~290/10~~	~~0074.9~~	~~1.016~~	~~1.023~~	~~1.040~~	~~0.196~~	~~215.6/06.4~~	~~123.2/20.0~~	~~322.6/68.9~~	~~216.1/16.1~~	~~119.5/22.0~~	~~339.3/62.3~~	~~12.9~~	~~14.5~~	~~13.7~~
	OR6	37.1838	27.8378	09	E.-Mid. Mio.	mud-marl	203/17	0620.0	1.003	1.003	1.006	0.110	295.6/03.1	205.4/05.0	057.6/84.2	115.7/13.9	206.7/04.0	312.6/75.5	43.5	44.9	36.5
	~~YT1~~	~~37.2353~~	~~28.1945~~	~~04~~	~~E. Mid. Mio.~~	~~mud-marl~~	~~075/11~~								No available data!						
	~~YT2~~	~~37.2632~~	~~28.1083~~	~~02~~	~~E. Mid. Mio.~~	~~mud-marl~~	~~000/12~~								No available data!						
	YT3	37.3641	28.0549	11	E.-Mid. Mio.	mud-marl	305/08	0030.3	1.024	1.069	1.100	0.492	310.9/07.6	041.2/02.3	147.9/82.1	311.9/06.7	221.3/05.7	091.2/81.2	55.1	55.1	08.3
E.-Mid. Mio.	**mean**			**29**	**E.-Mid. Mio.**		**~230/09**	**0211.0**	**1.016**	**1.030**	**1.049**	**0.128**	**319.7/05.2**	**049.7/00.1**	**141.3/84.8**	**322.1/03.9**	**231.7/06.0**	**085.1/82.9**	**57.2**	**57.2**	**11.7**
Tavas	TVS1	37.6254	29.0066	32	Lt. Mio.	mud-marl	+	1650.0	1.003	1.006	1.009	0.370	158.5/02.1	248.5/00.6	355.4/87.8	158.5/02.1	248.5/00.6	355.4/87.8	77.0	77.0	18.4
	TVS2	37.5142	28.8237	28	Lt. Mio.	mud-marl	203/31	1690.0	1.010	1.027	1.039	0.425	287.3/16.2	193.4/13.2	066.2/68.9	107.4/14.6	201.7/16.2	337.4/67.9	15.7	16.0	09.9
	TVS3	37.5581	28.7865	22	Lt. Mio.	mud-marl	+	1230.0	1.001	1.002	1.003	0.090	067.7/07.4	337.2/03.9	219.5/81.6	067.7/07.4	337.2/03.9	219.5/81.6	60.2	60.2	34.9
	~~TVS4~~	~~37.5345~~	~~28.6366~~	~~20~~	~~Lt. Mio.~~	~~mud-marl~~	~~+~~	~~0002.9~~	~~3.040~~	~~1.111~~	~~1.332~~	~~0.192~~	~~172.4/76.3~~	~~285.1/05.4~~	~~016.3/12.6~~	~~172.4/76.3~~	~~285.1/05.4~~	~~016.3/12.6~~	~~27.0~~	~~36.4~~	~~31.4~~
	TVS5	37.4681	28.6498	16	Lt. Mio.	lmst	142/06	0095.7	1.012	1.042	1.057	0.560	330.0/14.1	060.5/02.2	159.3/75.7	328.4/14.9	060.6/08.2	178.5/73.0	58.9	58.8	10.7
	KL1	37.2711	28.6523	12	Ol.-E.Mio.	mud-marl	158/26	0341.0	1.005	1.019	1.025	0.569	171.6/40.4	078.9/03.2	345.1/49.4	189.0/30.3	080.4/28.7	316.0/45.8	06.4	06.4	03.0
	KL2	37.2707	28.6187	17	Ol.-E.Mio.	mud-marl	044/55	1110.0	1.007	1.092	1.112	0.853	206.8/32.4	078.1/44.6	316.5/28.0	188.2/05.9	097.7/04.3	331.7/82.7	56.1	56.0	10.1
	KL3	37.2773	28.6246	29	E.Mio.	mud-marl	056/34	2260.0	1.004	1.052	1.063	0.858	210.1/30.6	099.4/31.0	334.5/43.6	198.4/12.2	107.2/05.6	353.2/76.5	26.5	26.6	06.2
	KL4	37.3237	28.6275	21	Ol.-E.Mio.	mud-marl	310/26	1210.0	1.023	1.077	1.107	0.522	343.2/05.6	076.1/27.4	242.62/61.9	162.6/08.7	308.8/79.6	308.8/79.6	05.5	05.5	03.7
	KL5	37.3719	28.5949	20	E.Mio.	mud-marl	214/11	0647.0	1.004	1.021	1.027	0.698	187.3/05.5	097.1/01.3	353.6/84.3	188.7/10.4	096.6/11.1	320.6/74.7	69.9	69.9	09.1

	~~KL6~~	~~37.3673~~	~~28.6562~~	~~16~~	~~E.Mio.~~	~~mud-marl~~	~~202/11~~	~~0011.1~~	~~1.071~~	~~1.103~~	~~1.192~~	~~0.305~~	~~328.7/08.1~~	~~237.2/10.6~~	~~095.3/76.6~~	~~328.7/08.1~~	~~238.3/04.2~~	~~048.1/85.8~~	~~54.9~~	~~54.8~~	~~24.2~~
Lt. Mio.	**mean**			**98**	**Lt. Mio.**		**~194/08**	**1310.0**	**1.006**	**1.017**	**1.024**	**0.354**	**295.4/11.4**	**204.8/02.9**	**100.6/78.2**	**100.1/05.3**	**190.2/01.1**	**292.1/84.5**	**37.5**	**37.8**	**31.3**
Ol.-E. Mio.				**99**	**Ol.-E.Mio.**		**~030/20**	**1280.0**	**1.009**	**1.054**	**1.069**	**0.719**	**059.9/13.8**	**158.4/31.0**	**309.0/55.4**	**173.5/10.5**	**082.7/04.5**	**329.6/78.6**	**30.3**	**30.3**	**8.5**
	~~PK1~~	~~38.0081~~	~~29.1435~~	~~12~~	~~Plio.~~	~~sand-marl~~	~~304/09~~	~~0021.8~~	~~1.028~~	~~1.022~~	~~1.052~~	~~-0.040~~	~~333.0/13.6~~	~~065.5/10.2~~	~~191.3/72.9~~	~~333.0/13.6~~	~~065.0/02.5~~	~~170.3/80.6~~	~~52.1~~	~~50.8~~	~~41.8~~
	CL1	37.8167	29.2797	14	Plio.	mud-marl	136/16	0414.0	1.010	1.026	1.038	0.415	194.7/08.3	285.5/05.8	050.1/79.8	014.9/5.4	105.1/02.4	218.9/84.1	23.1	23.2	9.6
	~~CL2~~	~~38.3445~~	~~29.5783~~	~~13~~	~~Plio.~~	~~mud-marl~~	~~+~~	~~0023.1~~	~~1.016~~	~~1.018~~	~~1.036~~	~~0.035~~	~~309.5/70.1~~	~~177.4/13.6~~	~~83.9 /14.2~~	~~309.5/70.1~~	~~177.4/13.6~~	~~83.9 /14.2~~	~~51.9~~	~~58.6~~	~~57.5~~
	CL3	38.5414	29.6563	15	Plio.	lmst	057/08	2280.0	1.006	1.022	1.029	0.477	053.7/01.2	143.8/07.2	314.5/82.7	053.9/1.6	323.9/00.8	206.6/88.2	37.3	37.2	14.6
Ulubey	~~UL1~~	~~38.3454~~	~~29.2171~~	~~12~~	Plio.	marl	~~+~~	~~0009.1~~	~~1.100~~	~~1.145~~	~~1.291~~	~~-0.111~~	~~117.0/11.5~~	~~359.6/66.2~~	~~211.4/20.5~~	~~117.0/11.5~~	~~359.6/66.2~~	~~211.4/20.5~~	~~46.5~~	~~62.6~~	~~62.2~~
	~~UL2~~	~~38.4193~~	~~29.2599~~	~~8~~	~~Plio.~~	~~marl~~	~~+~~	~~0004.7~~	~~1.055~~	~~1.076~~	~~1.142~~	~~0.010~~	~~75.00/37.1~~	~~187.6/26.9~~	~~303.8/41.1~~	~~75.00/37.1~~	~~187.6/26.9~~	~~303.8/41.1~~	~~47.9~~	~~47.9~~	~~45.1~~
	UL4	38.3245	29.1011	15	Plio.	mud-marl	+	2090.0	1.005	1.035	1.044	0.576	222.3/04.1	132.0/05.3	349.9/83.2	222.3/4.1	132.0/05.3	349.9/83.2	25.7	25.7	7.3
	~~UL5~~	~~38.1230~~	~~29.0384~~	~~15~~	~~Plio.~~	~~sand-marl~~	~~136 / 10~~	~~0009.2~~	~~1.070~~	~~1.054~~	~~1.139~~	~~0.111~~	~~280.0/16.9~~	~~182.7/22.7~~	~~043.4/61.6~~	~~278.0/10.9~~	~~185.0/15.3~~	~~042.1/71.1~~	~~28.8~~	~~19.9~~	~~30.5~~
	UL6	38.0457	28.9604	13	Plio.	sand-marl	+	1800.0	1.003	1.003	1.006	-0.057	160.2/22.0	307.9/64.5	065.1/12.3	160.2/22.0	307.9/64.5	065.1/12.3	39	39.1	17.3
Plio.	**mean**			**57**	**Plio.**		**~047/03**	**1660.0**	**1.006**	**1.022**	**1.028**	**0.366**	**198.4/06.5**	**108.3/01.4**	**006.1/83.3**	**200.2/00.3**	**110.2/01.9**	**300.3/88.1**	**46.6**	**46.6**	**11.5**
										REGIONAL											
Lt. Mio.-Plio.	**mean**			**784**	**Lt. Mio.-Plio.**			**0612.0**	**1.006**	**1.018**	**1.024**	**0.382**	**069.5/02.1**	**159.6/01.7**	**288.2/87.3**	**072.6/00.6**	**342.5/01.2**	**187.5/88.6**	**72.0**	**72.0**	**18.0**
Ol.-Mid. Mio.	**mean**			**599**	**Ol.-M. Mio.**			**0771.0**	**1.016**	**1.033**	**1.050**	**0.305**	**325.2/09.2**	**233.2/12.1**	**091.5/74.7**	**145.9/07.4**	**236.4/03.6**	**352.2/81.7**	**40.0**	**40.1**	**20.7**